

On the Convergence of Interior-Point Methods for Bound-Constrained Nonlinear Optimization Problems with Noise

Shima Dezfulian*

Andreas Wächter †

Abstract

We analyze the convergence properties of a modified barrier method for solving bound-constrained optimization problems where evaluations of the objective function and its derivatives are affected by bounded and non-diminishing noise. The only modification compared to a standard barrier method is a relaxation of the Armijo line-search condition. We prove that the algorithm generates iterates at which the size of the barrier function gradient eventually falls below a threshold that converges to zero if the noise level converges to zero. Based on this result, we propose a practical stopping test that does not require estimates of unknown problem parameters and identifies iterations in which the theoretical threshold is reached. We also analyze the local convergence properties of the method when noisy second derivatives are used. Under a strict-complementarity assumption, we show that iterates stay in a neighborhood around the optimal solution once it is entered. The neighborhood is defined in a scaled norm that becomes narrower for variables with active bound constraints as the barrier parameter is decreased. As a consequence, we show that active bound constraints can be identified despite noise. Numerical results demonstrate the effectiveness of the stopping test and illustrate the active-set identification properties of the method.

Key words. Interior-point method, Noisy optimization, Nonlinear Optimization, Nonconvex Optimization

AMS subject classifications. 65K05, 49M37, 90C53, 90C30, 90C51

1 Introduction

Interior-point methods are some of the most powerful techniques for solving nonlinear optimization problems with general equality and inequality constraints. They enjoy convergence guarantees in the non-noisy setting under conditions often satisfied in practice. However, when applied to problems where the function or constraints can only be evaluated with noise, their performance can be erratic. It is therefore natural to ask if the interior-point framework can be adapted to the noisy setting or if it is intrinsically unsuitable in this case.

In this paper, as a first step towards understanding the impact of noise in the interior-point framework, we focus on bound-constrained optimization problems

$$\min_{x \in \mathbb{R}^n} f(x) \quad \text{s.t.} \quad x \geq 0, \quad (1.1)$$

*(dezfulian@u.northwestern.edu) Department of Industrial Engineering and Management Sciences, Northwestern University

†(andreas.waechter@northwestern.edu) Department of Industrial Engineering and Management Sciences, Northwestern University

where $f : \mathbb{R}^n \rightarrow \mathbb{R}$ is continuously differentiable. We consider the standard barrier approach, where the only modification is a natural relaxation of the Armijo line-search condition.

In this paper, we assume that noise is persistent and cannot be diminished, in other words, it is outside the control of the user. Therefore, the convergence to the exact solution cannot be guaranteed and we present instead convergence results to neighborhoods with small barrier function gradients. We also assume that an estimate of the noise level in the function is available. We argue that this is natural since knowledge of the noise level is necessary to determine if a problem is satisfactorily solved and is required to ensure that certain computations within the algorithm are not contaminated by noise.

Applications of nonlinear programming in which the function and/or constraints contain noise abound. We refer the reader to the examples given in [16] involving robust design in the presence of stochastic noise, and to [14] for examples involving (deterministic) computational error. Interest in solving noisy nonlinear problems has been receiving increasing attention [1, 2, 3, 10, 11, 12, 15, 18, 19, 20, 23, 28].

1.1 Contributions

Our global convergence results are based on [1] which analyzes the behavior of line-search methods for unconstrained optimization with relaxed Armijo conditions in the presence of bounded noise. The analysis in [1] does not immediately apply in our setting because the required assumption that the objective function is bounded is violated by the log-barrier term. In addition, the analysis in [1] focuses on the gradient descent method, while we permit more general choices of the Hessian matrix, including second-derivatives. Our global convergence result is stated similarly to that in [18] and shows that eventually the stationary measure (the barrier objective gradients in our setting) must become small. The thresholds in [18] are defined in terms of unknown problem-dependent quantities and cannot be used as a practical stopping test. Overcoming this deficiency, we present a novel termination test that does not depend on unknown parameters and permits the user to recognize when the algorithm reaches the level of accuracy predicted by the global analysis. The effectiveness of this test is confirmed with numerical experiments.

Our local convergence analysis shows that locally the iterates converge at a quadratic-linear-type rate when noisy second-derivatives are used for a non-degenerate instance, similar to [13]. However, the analysis in [13] is not immediately applicable because the Hessian of the barrier function becomes unbounded as variables approach their bounds. We overcome this by utilizing a scaled norm, and we also prove the existence of a neighborhood around an optimal solution inside which the iterates are confined once it is entered. The particular scaling also allows us to argue that the method is able to identify which of the bound constraints are active at the solution as the barrier parameter goes to zero, despite the presence of noise. We present numerical results that demonstrate the identification of the active set.

1.2 Literature Review

Nonlinear optimization problems in the presence of noise have received increasing interest in recent years. In particular, recent research has focused on designing noise-tolerant algorithms based on certain assumptions about noise and its properties. Many of these studies aim to modify existing algorithms to obtain convergence guarantees.

Unconstrained problems with noisy function and gradient evaluations are studied in [1, 2, 4, 8, 12, 19, 21, 22, 23, 28]. They can be grouped into two categories: those that consider stochastic noise [2, 4, 8, 12, 19, 21] and those that consider bounded and non-diminishing noise [1, 22, 23, 28].

Since our assumptions align with the second category we provide a brief overview of them here. In [1], linear convergence of the gradient-descent algorithm with a relaxed Armijo line-search to a neighborhood of the solution for non-noisy problems is proved when the objective function is strongly convex. In [23], a modification of the trust-region algorithm that relaxes the numerator and denominator of the actual-to-predicted-reduction ratio is introduced. This modification guarantees convergence to a neighborhood of the non-noisy solution. In [28], a modification of the BFGS algorithm with a specialized Armijo-Wolfe line-search is proposed and convergence guarantees to a neighbourhood of the solution are provided.

Noisy equality-constrained optimization problems are studied in [3, 10, 18]. In [3], it is assumed that the evaluations of the objective function and its gradient are contaminated with a stochastic noise; however, equality constraint evaluations are deterministic. In this context, a modification of the line-search SQP algorithm is proposed that replaces the traditional line search with a step-size selection scheme based on Lipschitz constants or their approximations. The algorithm achieves global convergence, in expectation, to a local solution. The work in [10] considers a similar problem setting as [3]; however, it allows inexact solutions for the subproblems. More relevant to our context, [18] considers the setting where the objective function, equality constraints, and all gradients are affected by a non-diminishing bounded noise. The authors propose a modification of the line-search SQP algorithm that relaxes the Armijo condition [17], similar to [1]. Convergence to a neighborhood of the solution is shown under the assumption that first-order steps are taken.

Noisy optimization methods for solving problems with both inequality and equality constraints are studied in [11, 15, 20], where noise is assumed to be stochastic. All of these works assume noisy objective function and deterministic constraint evaluations and propose a modification of the SQP algorithm. Convergence in expectation [11] and almost sure convergence [15, 20] are established in this setting.

In this paper, we aim to design a noise-tolerant interior-point algorithm. In the deterministic setting, interior-point methods have been extensively studied and proven successful for solving very large-scale nonlinear optimization problems with equality and inequality constraints. As one of the first references, [29] considers a primal-dual line-search interior-point algorithm and provides global convergence to a local solution. Trust-region interior-point methods are studied, for example, in [6, 7, 30] and a convergence proof is provided in [6, 30]. A line-search filter interior-point algorithms are studied in [25, 26] and convergence proof of such algorithms is provided in [25].

In a setting with stochastic noise, an interior-point algorithm for solving bound-constrained problems is proposed and analyzed [9]. The algorithm proposed in [9] deviates more significantly from the standard interior-point framework than our work, as it does not employ the fraction-to-the-boundary rule; instead, it suggests a strategy that maintains the iterates within an inner neighborhood of the feasible region.

1.3 Notation

The sets of real numbers, n -dimensional real vectors, and n -by- m -dimensional real matrices are denoted by \mathbb{R} , \mathbb{R}^n , and $\mathbb{R}^{n \times m}$, respectively. The sets of nonnegative and positive real numbers are denoted by $\mathbb{R}_{\geq 0}$ and $\mathbb{R}_{> 0}$, respectively. The set of nonnegative integers is denoted by $\mathbb{N} := \{0, 1, \dots\}$ and we define $[n] := \{1, \dots, n\}$ for any $n \in \mathbb{N} \setminus \{0\}$. The identity matrix is denoted as I , and the vector of all ones is denoted as \mathbf{e} , where in each case the size of the object is determined by the context. We write $v_i \in \mathbb{R}$ to denote the i th element of a vector $v \in \mathbb{R}^n$ for all $i \in [n]$ and $v_k \in \mathbb{R}^n$ to denote the value of vector $v \in \mathbb{R}^n$ in iteration $k \in \mathbb{N}$ of the algorithm. In addition, $v_{k,i} \in \mathbb{R}$ denotes the i th element of vector $v_k \in \mathbb{R}^n$ in iteration $k \in \mathbb{N}$ of the algorithm, for all $i \in [n]$. For any vector $v \in \mathbb{R}^n$ we write $V \in \mathbb{R}^{n \times n}$ to denote $\text{diag}(v)$. The ℓ_2 -norm of any vector $v \in \mathbb{R}^n$ is denoted by $\|v\|$

and the induced 2-norm of any matrix $M \in \mathbb{R}^{m \times n}$ is denoted by $\|M\|$. The minimum and maximum eigenvalues of a matrix $M \in \mathbb{R}^{n \times n}$ are respectively denoted by $\sigma_{\min}(M)$ and $\sigma_{\max}(M)$. Given two symmetric matrices M_1 and M_2 in $\mathbb{R}^{n \times n}$, we write $M_1 \succ M_2$ and $M_1 \succeq M_2$ to denote $M_1 - M_2$ is positive definite and positive semi-definite, respectively. For a positive definite matrix $M \succ 0$ and a vector v , we use $\|v\|_M$ to denote $\sqrt{v^T M v}$. If $v_1 \in \mathbb{R}^{n_1}$ and $v_2 \in \mathbb{R}^{n_2}$, we write (v_1, v_2) to denote $(v_1^T, v_2^T)^T$. A fraction with a positive, finite numerator and a zero denominator evaluates to ∞ .

1.4 Organization

The formulation of the barrier subproblem and an algorithm for solving instances with noisy function evaluations are presented in Section 2. The global convergence analysis for solving the barrier subproblem is presented in Section 3, and local convergence is analyzed in Section 4. Numerical experiments are discussed in Section 5 and concluding remarks are given in Section 6.

2 An interior point method with noisy function evaluations

The analysis of interior-point methods for problems with general equality and inequality constraints is rather complex due (in part) to the complicated mechanisms of globalization techniques based on penalty functions or filters. Thus, in this paper, we consider the simpler setting of bound-constrained optimization (1.1), where the main design questions can be studied more directly and the numerical results are easier to analyze. In this case, the globalization mechanism reduces to a line search for the barrier objective function.

2.1 Barrier methods

In order to solve problem (1.1) using an interior-point or barrier algorithm, we define the *barrier subproblem*

$$\min_{x \in \mathbb{R}^n} \varphi^\mu(x) := f(x) - \mu \sum_{i=1}^n \log(x_i), \quad (2.1)$$

for a given barrier parameter $\mu \in \mathbb{R}_{>0}$. The main idea behind interior-point methods is to solve, often only to a certain tolerance, a sequence of barrier problems (2.1) for a decreasing sequence of barrier parameters that converges to zero.

Before introducing our algorithm that is able to handle the situation in which only noisy estimates of f and its derivatives are available, let us first recall some basic facts about barrier methods. We start with the primal-dual formulation of the necessary first-order optimality conditions for the barrier problem (2.1).

Theorem 2.1 ([17]). *Suppose f is continuously differentiable and let $\mu \in \mathbb{R}_{>0}$. If $x_*^\mu \in \mathbb{R}_{>0}^n$ is a local minimizer of (2.1), then there exists a vector $z_*^\mu \in \mathbb{R}_{>0}^n$ so that*

$$\begin{aligned} \nabla f(x) - z &= 0, \\ Xz &= \mu \mathbf{e}, \end{aligned} \quad (2.2)$$

holds with $x = x_*^\mu$ and $z = z_*^\mu$.

From this, one concludes $z_*^\mu = \mu(X_*^\mu)^{-1} \mathbf{e}$. The following assumption and theorem states sufficient second-order optimality conditions for the *original* problem (1.1), as well as the local existence of a central path.

Assumption 2.2. f is twice continuously differentiable. Let $x_*^0 \in \mathbb{R}_{\geq 0}^n$ and $z_*^0 \in \mathbb{R}_{\geq 0}^n$ be such that (i) (2.2) holds for $\mu = 0$, $x = x_*^0$, and $z = z_*^0$; (ii) strict complementarity holds, i.e., $x_*^0 + z_*^0 > 0$ for each $i \in [n]$; and (iii) the reduced Hessian $H_{*,\mathcal{II}}^0$ —with $H_*^0 = \nabla^2 f(x_*^0)$ and $\mathcal{I} = \{i \in [n] : x_{*,i}^0 > 0\}$ —is positive definite, i.e., $\sigma_{\mathcal{I}}^H = \sigma_{\min}(H_{*,\mathcal{II}}^0) > 0$.

For later reference, we also define $\mathcal{A} = [n] \setminus \mathcal{I}$.

Theorem 2.3 ([17]). *Suppose Assumption 2.2 holds. Then x_*^0 is a strict local minimizer of (1.1).*

Theorem 2.4 ([27]). *Suppose Assumption 2.2 holds. Then there exists $\hat{\mu} \in \mathbb{R}_{> 0}$ and a continuously differentiable primal-dual path $\phi(\mu) : [0, \hat{\mu}] \rightarrow \mathbb{R}^n \times \mathbb{R}^n$ so that $\phi(\mu) = (x_*^\mu, z_*^\mu)$ where x_*^μ and z_*^μ satisfy (2.2) with $x = x_*^\mu$ and $z = z_*^\mu$ for all $\mu \in [0, \hat{\mu}]$. Furthermore, there exists $\theta_\mu \in (0, 1)$ such that for all $i \in \mathcal{I}$ and $\mu \in [0, \hat{\mu}]$*

$$\theta_\mu \mu \leq |x_{*,i}^\mu - x_{*,i}^0| \leq \frac{1}{\theta_\mu} \mu,$$

where $x_{*,i}^\mu$ denotes the i th element of x_*^μ .

2.2 A line-search method for solving the barrier problem with noisy function evaluations

In this paper we assume that we have only access to noisy evaluations of f , its gradient $g := \nabla f$, and potentially its Hessian $H := \nabla^2 f$. The noisy evaluations of f and g are denoted by \tilde{f} and \tilde{g} . We further assume that the evaluation noise is bounded and non-diminishing.

Assumption 2.5. *Let \tilde{f} and \tilde{g} denote noisy evaluations of f and g , respectively. There exist constants $\epsilon_f, \epsilon_g \in \mathbb{R}_{\geq 0}$ such that for all $x \in \mathbb{R}^n$*

$$\tilde{f}(x) := f(x) + \epsilon_f(x), \text{ with } |\tilde{f}(x) - f(x)| = |\epsilon_f(x)| \leq \epsilon_f, \quad (2.3)$$

$$\tilde{g}(x) := g(x) + \epsilon_g(x), \text{ with } \|\tilde{g}(x) - g(x)\| = \|\epsilon_g(x)\| \leq \epsilon_g. \quad (2.4)$$

Here $\epsilon_f(x) \in \mathbb{R}$ denotes the error in the evaluation of $f(x)$ and $\epsilon_g(x) \in \mathbb{R}^n$ the component-wise errors in the evaluation of $g(x)$.

Even though we did not write it this way, the error terms $\epsilon_f(x)$ and $\epsilon_g(x)$ may not be deterministic, i.e., the oracle providing $\tilde{f}(x)$ and $\tilde{g}(x)$ may result in different values even if x is unchanged. We chose this notation to simplify the presentation.

In many practical applications, noise is bounded. Consider an engineering system whose performance we want to optimize, but that contains uncertainty in some of its physical parameters. By simulating it, we obtain an optimization problem with noisy evaluations, and if the decision variables are bounded, we can assume that the system response is always bounded [16]. A similar situation may arise if $\tilde{f}(x)$ is obtained by a complicated numerical procedure that results in a bounded round-off error.

In this section, we assume that the barrier parameter $\mu \in \mathbb{R}_{> 0}$ is fixed. As we discuss the algorithm for solving problem (2.1) and provide its convergence analysis, we use the superscript μ to emphasize the dependence on the barrier parameter. In the standard barrier method, subproblem (2.1) is solved by a Newton-like method, starting from a feasible point x_0^μ . We let \hat{H}_k^μ denote a real symmetric matrix (typically attempting to approximate $\nabla^2 f(x_k^\mu)$) and define

$$\hat{G}_k^\mu := \hat{H}_k^\mu + \mu(X_k^\mu)^{-2}, \quad (2.5)$$

as an approximation of the Hessian of the barrier function, $\nabla^2 \varphi^\mu(x_k^\mu)$. For our approach, it is crucial that the values and derivatives of the log-barrier terms are not approximated since they can easily be computed exactly.

We can now outline the barrier algorithm. In iteration k with an iterate x_k , the search direction d_k is calculated as

$$d_k = -(\hat{G}_k^\mu)^{-1} \nabla \tilde{\varphi}^\mu(x_k^\mu), \quad (2.6)$$

where, by slight abuse of notation, we define $\nabla \tilde{\varphi}^\mu(x) = \tilde{g}(x) - \mu X^{-1} \mathbf{e}$. The next iterate is computed as, $x_{k+1}^\mu = x_k^\mu + \alpha_k d_k$ for some step size $\alpha_k \in (0, 1]$.

In order to ensure the strict feasibility of the iterates, i.e., $x_k^\mu > 0$, the step size α_k is chosen to satisfy the *fraction-to-the-boundary rule*, i.e., $\alpha_k \in (0, \alpha_k^{\max}]$, where

$$\alpha_k^{\max} := \max \{ \alpha \in (0, 1] : x_k^\mu + \alpha d_k \geq (1 - \tau) x_k^\mu \}, \quad (2.7)$$

for some fixed parameter $\tau \in (0, 1)$. Furthermore, to force a decrease in the barrier function, the step size α_k is required to satisfy the *relaxed Armijo condition* [1] with parameter $\nu \in (0, \frac{1}{2})$ and relaxation ϵ_R ,

$$\tilde{\varphi}^\mu(x_k^\mu + \alpha_k d_k) \leq \tilde{\varphi}^\mu(x_k^\mu) + \nu \alpha_k \nabla \tilde{\varphi}^\mu(x_k^\mu)^T d_k + \epsilon_R, \quad (2.8)$$

where $\epsilon_R > 2\epsilon_f$ and $\tilde{\varphi}^\mu(x) = \tilde{f}(x) - \mu \sum_{i=1}^n \log(x_i)$. Note that the line search cannot fail due to the definition of ϵ_R since (2.8) is satisfied for all sufficiently small α_k by the continuity of φ^μ . The method is summarized in Algorithm 1. Its convergence proof is provided in the next section.

Algorithm 1 : Relaxed Armijo line-search for solving barrier subproblem (2.1)

Require: $\nu \in (0, \frac{1}{2})$; $\epsilon_R > 2\epsilon_f$; $\tau \in (0, 1)$; $\mu \in \mathbb{R}_{>0}$; initial iterate $x_0^\mu \in \mathbb{R}^n$.

- 1: **for** $k = 0, 1, \dots$ **do**
 - 2: Choose \hat{G}_k^μ by (2.5) and compute d_k by (2.6).
 - 3: Set $\alpha_k \leftarrow \alpha_k^{\max}$ with α_k^{\max} from (2.7).
 - 4: **while** α_k does not satisfy (2.8) **do**
 - 5: $\alpha_k \leftarrow \frac{1}{2} \alpha_k$.
 - 6: **end while**
 - 7: Set $x_{k+1}^\mu \leftarrow x_k^\mu + \alpha_k d_k$.
 - 8: **end for**
-

To ensure that the step d_k in (2.6) can be computed, we make the following assumption about \hat{G}_k^μ .

Assumption 2.6. \hat{G}_k^μ is uniformly positive definite, i.e., there exists $\hat{\sigma}_l^G \in \mathbb{R}_{>0}$ such that for all $k \in \mathbb{N}$

$$\sigma_{\min}(\hat{G}_k^\mu) \geq \hat{\sigma}_l^G. \quad (2.9)$$

This assumption is not very restrictive. In Lemma 4.6 we show that (2.9) holds if the sufficient second-order optimality conditions (Assumption 2.2) are satisfied, μ is sufficiently small, and \hat{H}_k^μ is a sufficiently accurate approximation of $\nabla^2 f(x_k^\mu)$.

3 Global convergence

In this section, we examine the convergence of Algorithm 1 for a fixed value of μ . Our work extends the results in [1] in several ways by (i) permitting an unbounded barrier objective function; (ii)

considering second-order (Newton-like) steps instead of gradient steps; and (iii) allowing nonconvex instead of only strongly convex functions. Furthermore, Section 3.2 introduces a practical termination test that could also be applied to the algorithm in [1].

It is well known that primal-dual interior-point methods (e.g., Algorithm 2 in Appendix E) perform much better in practice than the primal method described above. The primal-dual method maintains iterates z_k^μ approximating the bound multipliers and calculates the search directions from (2.6) with

$$\hat{G}_k^\mu = \hat{H}_k^\mu + Z_k^\mu (X_k^\mu)^{-1}, \quad (3.1)$$

instead of (2.5). For simplicity, we analyze in this section the primal method using (2.5), but the results hold also for the primal-dual method if a safeguard is implemented like in [26] that ensures that z_k^μ has positive entries and does not deviate arbitrarily far from $\mu(X_k^\mu)^{-1}\mathbf{e}$ (see (E.5) in Appendix E.) The only difference is that the threshold δ_x in Lemma 3.4 might be smaller than in the primal case.

To simplify the notation, we let $\varphi_k^\mu = \varphi^\mu(x_k^\mu)$ and $\nabla\varphi_k^\mu = \nabla\varphi^\mu(x_k^\mu)$ and use similar simplifications for the noisy quantities.

3.1 Global convergence analysis

In addition to Assumptions 2.5 and 2.6, we require the following assumptions.

Assumption 3.1. *There exists an open set $\mathcal{X} \subset \mathbb{R}^n$ such that $\{x_k^\mu + \alpha d_k : \alpha \in [0, 1]\} \subset \mathcal{X}$ for all k , f is differentiable and bounded below on \mathcal{X} and the gradient ∇f is bounded and Lipschitz continuous with constant $L_g \in \mathbb{R}_{>0}$ over \mathcal{X} , i.e., for all $x, y \in \mathcal{X}$ one has*

$$\|g(x) - g(y)\| \leq L_g \|x - y\|.$$

Assumption 3.2. *The Hessian approximation \hat{H}_k is uniformly bounded.*

In the following, we prove some preliminary results before stating the main theorem. In addition, for the remainder of this section, we assume that Assumptions 2.5, 2.6, 3.1, and 3.2 hold for all the lemmas and theorems stated and proved herein.

Lemma 3.3. *Let $x_k^\mu \in \mathbb{R}_{>0}^n$, $d_k \in \mathbb{R}^n$, τ be the fraction-to-the-boundary parameter in (2.7), and suppose $\alpha \leq \alpha_k^{\max}$. Then*

$$-\left(\sum_{i=1}^n \log(x_{k,i}^\mu + \alpha d_{k,i}) - \sum_{i=1}^n \log(x_{k,i}^\mu) - \alpha \sum_{i=1}^n \frac{d_{k,i}}{x_{k,i}^\mu} \right) \leq \alpha^2 \frac{1}{1-\tau} \|(X_k^\mu)^{-1} d_k\|^2$$

Proof. The proof is similar to that of Lemma 4 in [6]. □

Lemma 3.4. *There exists a constant $\delta_x \in \mathbb{R}_{>0}$ such that $x_k^\mu \geq \delta_x \mathbf{e}$ for all k .*

Proof. This claim was proven as Theorem 3 in [25]. □

Lemma 3.5. *There exists $\Delta_d \in \mathbb{R}_{>0}$ such that $\|d_k\| \leq \Delta_d$ for all k .*

Proof. By Assumptions 2.6, together with Lemma 3.4 one finds $\|d_k\| \leq \|(\hat{G}_k^\mu)^{-1}\| \|\nabla\tilde{\varphi}^\mu(x_k^\mu)\| \leq \frac{1}{\hat{\sigma}_l^\mu} \|\tilde{g}(x_k^\mu) - \mu(X_k^\mu)^{-1}\mathbf{e}\| \leq \frac{1}{\hat{\sigma}_l^\mu} \left(\Delta_g + \varepsilon_g + \frac{\mu}{\delta_x} \right)$, where the upper bound Δ_g on $\|g(x_k^\mu)\|$ exists by Assumption 3.1. □

Lemma 3.6. *Let us define*

$$\bar{\alpha} := \min \left\{ 1, \frac{\tau \delta_x}{\Delta_d}, \frac{\hat{\sigma}_l^G}{L_g + \frac{2\mu}{(1-\tau)\delta_x^2}} \right\}, \quad (3.2)$$

then for any k that $\bar{\alpha} \leq \alpha_k^{\max}$ and for any $\alpha \in (0, \bar{\alpha})$

$$\varphi^\mu(x_k^\mu + \alpha d_k) - \varphi^\mu(x_k^\mu) \leq -\frac{\alpha}{2} \|\nabla \varphi^\mu(x_k^\mu)\|_{(\hat{G}_k^\mu)^{-1}}^2 + \frac{\alpha}{2} \|\varepsilon_g(x_k^\mu)\|_{(\hat{G}_k^\mu)^{-1}}^2.$$

Proof. Consider a fixed iteration k . Then, from (2.7), $\alpha_k^{\max} = 1$ or $\alpha_k^{\max} = \frac{-\tau x_{k,i}^\mu}{d_{k,i}}$ with $d_{k,i} < 0$ for some i . Using Lemmas 3.4 and 3.5, we conclude that $\bar{\alpha} \leq \alpha_k^{\max}$.

By Taylor's theorem, $\alpha \leq \bar{\alpha} \leq \alpha_k^{\max}$, and Lemma 3.3, one finds

$$\begin{aligned} \varphi^\mu(x_k^\mu + \alpha d_k) - \varphi^\mu(x_k^\mu) &= f(x_k^\mu + \alpha d_k) - \mu \sum_{i=1}^n \log(x_{k,i}^\mu + \alpha d_{k,i}) \\ &\quad - f(x_k^\mu) + \mu \sum_{i=1}^n \log(x_{k,i}^\mu) \\ &\leq \alpha \nabla \varphi^\mu(x_k^\mu)^T d_k + \frac{\alpha^2}{2} d_k^T \check{H}_k d_k + \frac{\mu}{1-\tau} \alpha^2 \|(X_k^\mu)^{-1} d_k\|^2 \\ &= \alpha \nabla \varphi^\mu(x_k^\mu)^T d_k + \frac{\alpha^2}{2} d_k^T \check{G}_k^\mu d_k \end{aligned} \quad (3.3)$$

where $\check{H}_k^\mu := \nabla^2 f(x_k^\mu + \check{\alpha} d_k)$ for some $\check{\alpha} \in (0, 1)$, and $\check{G}_k^\mu := \check{H}_k^\mu + \frac{2\mu}{1-\tau} (X_k^\mu)^{-2}$. By substituting d_k from (2.6) one has

$$\begin{aligned} &\varphi^\mu(x_k^\mu + \alpha d_k) - \varphi^\mu(x_k^\mu) \\ &\leq -\alpha \nabla \varphi^\mu(x_k^\mu)^T (\hat{G}_k^\mu)^{-1} (\nabla \varphi^\mu(x_k^\mu) + \varepsilon_g(x_k^\mu)) \\ &\quad + \frac{\alpha^2}{2} (\nabla \varphi^\mu(x_k^\mu) + \varepsilon_g(x_k^\mu))^T (\hat{G}_k^\mu)^{-1} \check{G}_k^\mu (\hat{G}_k^\mu)^{-1} (\nabla \varphi^\mu(x_k^\mu) + \varepsilon_g(x_k^\mu)) \\ &= -\frac{\alpha}{2} \nabla \varphi^\mu(x_k^\mu)^T (\hat{G}_k^\mu)^{-1} \left(2\hat{G}_k^\mu - \alpha \check{G}_k^\mu \right) (\hat{G}_k^\mu)^{-1} \nabla \varphi^\mu(x_k^\mu) \\ &\quad + \frac{\alpha^2}{2} \varepsilon_g(x_k^\mu)^T (\hat{G}_k^\mu)^{-1} \check{G}_k^\mu (\hat{G}_k^\mu)^{-1} \varepsilon_g(x_k^\mu) \\ &\quad - \alpha \nabla \varphi^\mu(x_k^\mu)^T (\hat{G}_k^\mu)^{-1} \left(\hat{G}_k^\mu - \alpha \check{G}_k^\mu \right) (\hat{G}_k^\mu)^{-1} \varepsilon_g(x_k^\mu). \end{aligned} \quad (3.4)$$

By Assumptions 3.1 and 2.6 and Lemma 3.4 we have

$$\hat{G}_k^\mu - \alpha \check{G}_k^\mu \succeq \left(\hat{\sigma}_l^G - \alpha \left(L_g + \frac{2\mu}{(1-\tau)\delta_x^2} \right) \right) I,$$

which implies that for any $\alpha \in (0, \bar{\alpha})$, $\hat{G}_k^\mu - \alpha \check{G}_k^\mu \succ 0$. Let $R_k^T R_k$ be the Cholesky factorization of $\hat{G}_k^\mu - \alpha \check{G}_k^\mu$ for such an α . Using the fact that $-v^T w \leq \frac{\|v\|^2}{2} + \frac{\|w\|^2}{2}$ for arbitrary vectors $v, w \in \mathbb{R}^n$, we have

$$\begin{aligned} &-\alpha \nabla \varphi^\mu(x_k^\mu)^T (\hat{G}_k^\mu)^{-1} \left(\hat{G}_k^\mu - \alpha \check{G}_k^\mu \right) (\hat{G}_k^\mu)^{-1} \varepsilon_g(x_k^\mu) \\ &\leq \frac{\alpha}{2} \left(\|R_k (\hat{G}_k^\mu)^{-1} \nabla \varphi^\mu(x_k^\mu)\|^2 + \|R_k (\hat{G}_k^\mu)^{-1} \varepsilon_g(x_k^\mu)\|^2 \right) \\ &\leq \frac{\alpha}{2} \nabla \varphi^\mu(x_k^\mu)^T (\hat{G}_k^\mu)^{-1} R_k^T R_k (\hat{G}_k^\mu)^{-1} \nabla \varphi^\mu(x_k^\mu) + \frac{\alpha}{2} \varepsilon_g(x_k^\mu)^T (\hat{G}_k^\mu)^{-1} R_k^T R_k (\hat{G}_k^\mu)^{-1} \varepsilon_g(x_k^\mu). \end{aligned}$$

Combining this with (3.4) we obtain

$$\begin{aligned}
& \varphi^\mu(x_k^\mu + \alpha d_k) - \varphi^\mu(x_k^\mu) \\
& \leq -\frac{\alpha}{2} \nabla \varphi^\mu(x_k^\mu)^T (\hat{G}_k^\mu)^{-1} \left(2\hat{G}_k^\mu - \alpha \check{G}_k^\mu - R_k^T R_k \right) (\hat{G}_k^\mu)^{-1} \nabla \varphi^\mu(x_k^\mu) \\
& \quad + \frac{\alpha}{2} \varepsilon_g(x_k^\mu)^T (\hat{G}_k^\mu)^{-1} \left(\alpha \check{G}_k^\mu + R_k^T R_k \right) (\hat{G}_k^\mu)^{-1} \varepsilon_g(x_k^\mu) \\
& = -\frac{\alpha}{2} \nabla \varphi^\mu(x_k^\mu)^T (\hat{G}_k^\mu)^{-1} \nabla \varphi^\mu(x_k^\mu) + \frac{\alpha}{2} \varepsilon_g(x_k^\mu)^T (\hat{G}_k^\mu)^{-1} \varepsilon_g(x_k^\mu) \\
& = -\frac{\alpha}{2} \|\nabla \varphi^\mu(x_k^\mu)\|_{(\hat{G}_k^\mu)^{-1}}^2 + \frac{\alpha}{2} \|\varepsilon_g(x_k^\mu)\|_{(\hat{G}_k^\mu)^{-1}}^2,
\end{aligned}$$

as desired. \square

For the next results, we define the noise-to-signal ratio β_k [1] as

$$\beta_k := \frac{\|\varepsilon_g(x_k^\mu)\|_{(\hat{G}_k^\mu)^{-1}}}{\|\nabla \varphi^\mu(x_k^\mu)\|_{(\hat{G}_k^\mu)^{-1}}}, \quad (3.5)$$

and observe that by Assumption 2.5 and triangle inequality, one finds

$$(1 - \beta_k) \|\nabla \varphi^\mu(x_k^\mu)\|_{(\hat{G}_k^\mu)^{-1}} \leq \|\nabla \tilde{\varphi}^\mu(x_k^\mu)\|_{(\hat{G}_k^\mu)^{-1}} \leq (1 + \beta_k) \|\nabla \varphi^\mu(x_k^\mu)\|_{(\hat{G}_k^\mu)^{-1}}. \quad (3.6)$$

Lemma 3.7. *If $\beta_k \leq \frac{1-2\nu}{1+2\nu}$ then the relaxed Armijo condition (2.8) holds for any $\alpha \in (0, \bar{\alpha})$ where $\bar{\alpha}$ is defined in (3.2).*

Proof. By Lemma 3.6 for any $\alpha \in (0, \bar{\alpha})$

$$\varphi^\mu(x_k^\mu + \alpha d_k) - \varphi^\mu(x_k^\mu) \leq -\frac{\alpha}{2} \|\nabla \varphi^\mu(x_k^\mu)\|_{(\hat{G}_k^\mu)^{-1}}^2 + \frac{\alpha}{2} \|\varepsilon_g(x_k^\mu)\|_{(\hat{G}_k^\mu)^{-1}}^2.$$

Hence, by Assumption 2.5, (3.5), and (3.6), one finds that for such an α

$$\begin{aligned}
\tilde{\varphi}^\mu(x_k^\mu + \alpha d_k) - \tilde{\varphi}^\mu(x_k^\mu) & \leq -\frac{\alpha}{2} \|\nabla \varphi^\mu(x_k^\mu)\|_{(\hat{G}_k^\mu)^{-1}}^2 + \frac{\alpha}{2} \|\varepsilon_g(x_k^\mu)\|_{(\hat{G}_k^\mu)^{-1}}^2 + 2\epsilon_f \\
& \leq -\frac{\alpha}{2} (1 - \beta_k^2) \|\nabla \varphi^\mu(x_k^\mu)\|_{(\hat{G}_k^\mu)^{-1}}^2 + 2\epsilon_f \\
& < -\frac{\alpha}{2} \frac{1-\beta_k}{1+\beta_k} \|\nabla \tilde{\varphi}^\mu(x_k^\mu)\|_{(\hat{G}_k^\mu)^{-1}}^2 + \epsilon_R,
\end{aligned} \quad (3.7)$$

where we used $\epsilon_R > 2\epsilon_f$ and (3.6) to obtain the last inequality. If $\beta_k \leq \frac{1-2\nu}{1+2\nu}$, then $-\frac{1}{2} \frac{(1-\beta_k)}{(1+\beta_k)} \leq -\nu$ and one finds

$$\tilde{\varphi}^\mu(x_k^\mu + \alpha d_k) - \tilde{\varphi}^\mu(x_k^\mu) < -\nu \alpha \|\nabla \tilde{\varphi}^\mu(x_k^\mu)\|_{(\hat{G}_k^\mu)^{-1}}^2 + \epsilon_R,$$

which together with (2.5) implies (2.8). \square

We can now state the global convergence result for Algorithm 1.

Theorem 3.8. *Let D be a symmetric positive-definite matrix and $\gamma \in (0, 1)$. Consider the set $\mathcal{C}(D, \nu, \gamma)$ defined as*

$$\mathcal{C}(D, \nu, \gamma) := \left\{ x \in \mathcal{X} : \|\nabla \tilde{\varphi}^\mu(x)\|_D \leq \max \left\{ \sqrt{\frac{\hat{\sigma}_u^D}{\hat{\sigma}_l^G}} \left(\frac{1+2\nu}{1-2\nu} + 1 \right) \epsilon_g, \sqrt{\hat{\sigma}_u^D} \sqrt{\frac{4\epsilon_f + 2\epsilon_R}{\gamma \bar{\alpha} \nu}} \right\} \right\} \quad (3.8)$$

where $\hat{\sigma}_u^D = \sup_k \left\| D^{1/2} \hat{G}_k^\mu D^{1/2} \right\|$ and $\bar{\alpha}$ is defined in (3.2). Then the iterates $\{x_k^\mu\}$ generated by Algorithm 1 enter $\mathcal{C}(D, \nu, \gamma)$ infinitely many times.

Proof. Let $\hat{k} \in \mathbb{N}$ and $k \geq \hat{k}$ so that $x_k^\mu \notin \mathcal{C}(D, \nu, \gamma)$. By the definition of $\mathcal{C}(D, \nu, \gamma)$

$$\|\nabla \tilde{\varphi}^\mu(x_k^\mu)\|_D > \sqrt{\frac{\hat{\sigma}_u^D}{\hat{\sigma}_l^G}} \left(\frac{1+2\nu}{1-2\nu} + 1 \right) \epsilon_g, \text{ and } \|\nabla \tilde{\varphi}^\mu(x_k^\mu)\|_D > \sqrt{\hat{\sigma}_u^D} \sqrt{\frac{4\epsilon_f + 2\epsilon_R}{\gamma\bar{\alpha}\nu}}. \quad (3.9)$$

The definition of $\hat{\sigma}_u^D$ implies $\|D^{1/2}(\hat{G}_k^\mu)^{1/2}\| \leq \sqrt{\hat{\sigma}_u^D}$. Since \hat{G}_k^μ is invertible, we have $\|\nabla \tilde{\varphi}^\mu(x_k^\mu)\|_D \leq \|D^{1/2}(\hat{G}_k^\mu)^{1/2}\| \|(\hat{G}_k^\mu)^{-1/2} \nabla \tilde{\varphi}^\mu(x_k^\mu)\|$. This, along with the first inequality in (3.9) implies

$$\begin{aligned} \sqrt{\hat{\sigma}_u^D} \|\nabla \tilde{\varphi}^\mu(x_k^\mu)\|_{(\hat{G}_k^\mu)^{-1}} &\geq \|\nabla \tilde{\varphi}^\mu(x_k^\mu)\|_D > \sqrt{\frac{\hat{\sigma}_u^D}{\hat{\sigma}_l^G}} \left(\frac{1+2\nu}{1-2\nu} + 1 \right) \epsilon_g \\ &\geq \sqrt{\hat{\sigma}_u^D} \left(\frac{1+2\nu}{1-2\nu} + 1 \right) \|\varepsilon_g(x_k^\mu)\|_{(\hat{G}_k^\mu)^{-1}}, \end{aligned} \quad (3.10)$$

because $\|\varepsilon_g(x_k^\mu)\|_{(\hat{G}_k^\mu)^{-1}} \leq 1/\sqrt{\hat{\sigma}_l^G} \cdot \epsilon_g$ and (2.9). By Assumption 2.5, we have $\|\nabla \tilde{\varphi}^\mu(x_k^\mu)\|_{(\hat{G}_k^\mu)^{-1}} \leq \|\varepsilon_g(x_k^\mu)\|_{(\hat{G}_k^\mu)^{-1}} + \|\nabla \varphi^\mu(x_k^\mu)\|_{(\hat{G}_k^\mu)^{-1}}$. Together this yields

$$\|\nabla \varphi^\mu(x_k^\mu)\|_{(\hat{G}_k^\mu)^{-1}} > \left(\frac{1+2\nu}{1-2\nu} \right) \|\varepsilon_g(x_k^\mu)\|_{(\hat{G}_k^\mu)^{-1}}. \quad (3.11)$$

Hence, by Lemma 3.7 and Assumption 2.5 one concludes that the backtracking line-search finds $\alpha_k > \bar{\alpha}/2$ satisfying the relaxed Armijo condition, that is

$$\begin{aligned} \varphi^\mu(x_k^\mu + \alpha_k d_k) - \varphi^\mu(x_k^\mu) &\leq \tilde{\varphi}^\mu(x_k^\mu + \alpha_k d_k) - \tilde{\varphi}^\mu(x_k^\mu) + 2\epsilon_f \\ &< -\frac{\bar{\alpha}}{2}\nu \|\nabla \tilde{\varphi}^\mu(x_k^\mu)\|_{(\hat{G}_k^\mu)^{-1}}^2 + 2\epsilon_f + \epsilon_R. \end{aligned} \quad (3.12)$$

The second inequality in (3.9), along with the first inequality in (3.10) yields

$$\|\nabla \tilde{\varphi}^\mu(x_k^\mu)\|_{(\hat{G}_k^\mu)^{-1}} > \sqrt{\frac{4\epsilon_f + 2\epsilon_R}{\gamma\bar{\alpha}\nu}},$$

which in combination with (3.12) implies

$$\varphi^\mu(x_k^\mu + \alpha_k d_k) - \varphi^\mu(x_k^\mu) < (1 - \frac{1}{\gamma})(2\epsilon_f + \epsilon_R) < 0.$$

Since φ is bounded below by Assumption 3.1, $x_k^\mu \notin \mathcal{C}(D, \nu, \gamma)$ cannot hold for all $k \geq \hat{k}$, where \hat{k} can be arbitrarily large. \square

This theorem presents a global convergence result in the sense that it states that the gradient is small for infinitely many iterations. The set $\mathcal{C}(D, \nu, \gamma)$ is defined in terms of the noisy gradient, but it can easily be transferred into a condition using the norm of the non-noisy gradient $\|\nabla \varphi^\mu(x_k^\mu)\|_D$, by adding ϵ_g to the right-hand side, multiplied by a constant that accounts for the difference between $\|\cdot\|_D$ and $\|\cdot\|$. Since $\gamma \in (0, 1)$ can be chosen arbitrarily close to one, an alternative way to state this result is that there exists a limit point of x_k^μ that is in $\mathcal{C}(D, \nu, 1)$.

Different choices for the norm $\|\cdot\|_D$ are possible, resulting in different conditions. For instance, for $D = I$, we have on the right-hand side $\hat{\sigma}_u^D = \max_k \|\hat{H}_k + \mu(X_k^\mu)^{-2}\|$, a quantity that converges to infinity as $\mu \rightarrow 0$ if $x_k^\mu \approx x_*^\mu$. (Recall that $\mu(X_*^\mu)^{-2} = Z_*^\mu(X_*^\mu)^{-1}$ due to (2.2).) At the same time, though, $\|\nabla \tilde{\varphi}^\mu(x_k^\mu)\| = \|\tilde{g}(x_k^\mu) - \mu(X_k^\mu)^{-1}\mathbf{e}\|$ is a bounded entity. This makes the result essentially meaningless for $D = I$ as $\mu \rightarrow 0$.

On the other hand, choosing $D = (X_*^\mu)^{-2}$ yields $\hat{\sigma}_u^D = \sup_k \|X_*^\mu \hat{H}_k X_*^\mu + \mu I\|$ and the spurious high curvature induced by the barrier term is neutralized, leaving behind a matrix that becomes a scaled version of the reduced Hessian as $\mu \rightarrow 0$. Finally, $D = G^\mu(x_*^\mu) = \nabla^2 f(x_*^\mu) + \mu(X_*^\mu)^{-2}$ provides a scale-invariant measure and, if $\hat{H}_k \approx \nabla^2 f(x_*^\mu)$, yields $\hat{\sigma}_u^D \approx 1$. This is what is used in the stopping test below.

3.2 A practical stopping test

In this section, having established the global convergence result in Theorem 3.8, we take our findings a step further by providing a practical stopping test for Algorithm 1. The practicality of this stopping test lies in the fact that it does not depend on unknown parameters such as $\hat{\sigma}_u^D$, $\hat{\sigma}_l^G$, and $\bar{\alpha}$. Instead, all these parameters have been replaced by their iteration-dependent counterparts which can be computed as the algorithm runs.

This result is formally presented in the following theorem.

Theorem 3.9. *There exists $k \in \mathbb{N}$ such that*

- (i) $\|\nabla\tilde{\varphi}^\mu(x_k^\mu)\|_{(\hat{G}_k^\mu)^{-1}} \leq T_{1,k}$, or
- (ii) $\|\nabla\tilde{\varphi}^\mu(x_k^\mu)\|_{(\hat{G}_k^\mu)^{-1}} > T_{1,k}$ and $\|\nabla\tilde{\varphi}^\mu(x_k^\mu)\|_{(\hat{G}_k^\mu)^{-1}} \leq T_{2,k}$,

where

$$T_{1,k} = \frac{1}{\sqrt{\hat{\sigma}_{l,k}^G}} \left(\frac{1+2\nu_k}{1-2\nu_k} + 1 \right) \epsilon_g \quad \text{and} \quad T_{2,k} = \sqrt{\frac{2\epsilon_f + \epsilon_R}{\gamma\alpha_k\nu_k}}, \quad (3.13)$$

$\gamma \in (0, 1)$ is a fixed constant that can be chosen arbitrarily close to one, $\hat{\sigma}_{l,k}^G = \sigma_{\min}(\hat{G}_k^\mu)$, and ν_k is an arbitrarily chosen scalar in $[\nu, \hat{\nu}_{1,k}]$, where

$$\hat{\nu}_{1,k} := \frac{\tilde{\varphi}(x_k) - \tilde{\varphi}(x_k + \alpha_k d_k) + \epsilon_R}{\alpha_k \|\nabla\tilde{\varphi}^\mu(x_k^\mu)\|_{(\hat{G}_k^\mu)^{-1}}^2} \geq \nu. \quad (3.14)$$

Furthermore, such iteration satisfies $x_k^\mu \in \mathcal{C}((\hat{G}_k^\mu)^{-1}, \nu_k, \gamma)$.

Proof. Suppose that $\|\nabla\tilde{\varphi}^\mu(x_k^\mu)\|_{(\hat{G}_k^\mu)^{-1}} > T_{2,k}$ for all $k \in \mathbb{N}$. Observe that $\hat{\nu}_{1,k}$ is the largest value of ν such that the Armijo condition (2.8) holds for the step size α_k in the k th iteration. Therefore, $\hat{\nu}_{1,k} \geq \nu$ and

$$\begin{aligned} \varphi^\mu(x_k^\mu + \alpha_k d_k) - \varphi^\mu(x_k^\mu) &\leq \tilde{\varphi}^\mu(x_k^\mu + \alpha_k d_k) - \tilde{\varphi}^\mu(x_k^\mu) + 2\epsilon_f \\ &\leq -\alpha_k \nu_k \|\nabla\tilde{\varphi}^\mu(x_k^\mu)\|_{(\hat{G}_k^\mu)^{-1}}^2 + 2\epsilon_f + \epsilon_R \\ &< \left(1 - \frac{1}{\gamma}\right) (2\epsilon_f + \epsilon_R) < 0, \end{aligned}$$

where we used the definition of $T_{2,k}$. But this cannot hold for all $k \in \mathbb{N}$ since φ^μ is bounded below. Hence, there exists $k \in \mathbb{N}$ such that $\|\nabla\tilde{\varphi}^\mu(x_k^\mu)\|_{(\hat{G}_k^\mu)^{-1}} \leq T_{2,k}$, and therefore one of the conditions (i) and (ii) must hold.

Next, let $k \in \mathbb{N}$ such that condition (i) or condition (ii) holds. If (i) holds, recall that $\hat{\sigma}_u^D = 1$ for $D = (\hat{G}_k^\mu)^{-1}$ and $\hat{\sigma}_{l,k}^G \geq \hat{\sigma}_l^G$. This implies that $T_{k,1}$ is not larger than the first term in the max-expression in (3.8), and therefore $x_k^\mu \in \mathcal{C}((\hat{G}_k^\mu)^{-1}, \nu_k, \gamma)$.

Now suppose that (ii) holds. Since $\hat{\sigma}_{l,k}^G = \sigma_{\min}(\hat{G}_k^\mu)$, one has $\frac{\epsilon_g}{\sqrt{\hat{\sigma}_{l,k}^G}} \geq \|\varepsilon_g(x_k^\mu)\|_{(\hat{G}_k^\mu)^{-1}}$. This, together with $\|\nabla\varphi^\mu(x_k^\mu)\|_{(\hat{G}_k^\mu)^{-1}} + \|\varepsilon_g(x_k^\mu)\|_{(\hat{G}_k^\mu)^{-1}} \geq \|\nabla\tilde{\varphi}^\mu(x_k^\mu)\|_{(\hat{G}_k^\mu)^{-1}}$ and the first inequality in (ii) implies

$$\|\nabla\varphi^\mu(x_k^\mu)\|_{(\hat{G}_k^\mu)^{-1}} + \|\varepsilon_g(x_k^\mu)\|_{(\hat{G}_k^\mu)^{-1}} > \left(\frac{1+2\nu_k}{1-2\nu_k} + 1 \right) \|\varepsilon_g(x_k^\mu)\|_{(\hat{G}_k^\mu)^{-1}},$$

and by (3.5), one has $\beta_k < \frac{1-2\nu_k}{1+2\nu_k}$. Since $\nu_k \geq \nu$, one also has that $\beta_k < \frac{1-2\nu}{1+2\nu}$. Hence, by Lemma 3.7 one concludes that (2.8) is satisfied with $\alpha_k > \frac{\bar{\alpha}}{2}$. Consequently, $T_{k,2}$ is not larger than the second term in the max-expression in (3.8), and the second inequality in (ii) yields $x_k^\mu \in \mathcal{C}((\hat{G}_k^\mu)^{-1}, \nu_k, \gamma)$. \square

Remark 3.10. This theorem can be used to define a practical termination test. During the run of the algorithm, we can check in each iteration whether condition (i) or (ii) in Theorem 3.9 holds. If that is the case, we can conclude that the noisy gradient of the barrier function at the current iterate x_k^μ is as small as we were able to prove in the theoretical convergence Theorem 3.8 (if we choose $\nu_k = \nu$), without the need to know the values of the parameters $\hat{\sigma}_l^G$ and $\bar{\alpha}$. Since these values are pessimistic uniform estimates, the use of the actual values $\hat{\sigma}_{l,k}^G$ and α_k in $T_{1,k}$ and $T_{k,2}$ typically results in a smaller final value of $\|\nabla\tilde{\varphi}^\mu(x_k^\mu)\|_{(\hat{G}_k^\mu)^{-1}}$ than what Theorem 3.8 predicts.

By keeping the choice of the Armijo condition parameter ν_k flexible, we can tighten the final tolerance even further. The tolerances $T_{1,k}$ and $T_{2,k}$ are monotonically increasing and decreasing, respectively, as ν_k becomes larger. To obtain the tightest bound we choose the value that balances the two tolerances, namely

$$\hat{\nu}_{2,k} := \frac{(2\epsilon_f + \epsilon_R)\hat{\sigma}_{l,k}^G + \gamma\alpha_k\epsilon_g^2 - \sqrt{\gamma^2\alpha_k^2\epsilon_g^4 + 2(2\epsilon_f + \epsilon_R)\hat{\sigma}_{l,k}^G\gamma\alpha_k\epsilon_g^2}}{2(2\epsilon_f + \epsilon_R)\hat{\sigma}_{l,k}^G}.$$

However, since the assumptions of Theorem 3.9 require that $\nu_k \in [\nu, \hat{\nu}_{1,k}]$, the tightest value we can choose (and use in our numerical experiments) is

$$\nu_k := \max\{\nu, \min\{\hat{\nu}_{1,k}, \hat{\nu}_{2,k}\}\}. \quad (3.15)$$

4 Local convergence

In this section, we examine the behavior of the iterates when they are close to a local optimal solution satisfying the second-order optimality conditions and when Newton-type steps are taken with a noisy approximation of the Hessian matrix. First, we derive in Section 4.1 a noisy version of a local quadratic convergence rate, presented in Theorem 4.11. This permits us to show in Section 4.2 the existence of “neighborhoods of confusion” around the optimal solution in which the iterates remain once entered. A significant effort is made to keep all constants independent of the barrier parameter μ because this allows us to eventually argue that interior-point methods can identify the active set (for non-degenerate problems) despite noise. We emphasize that we do not require that the problem is convex.

Throughout this section, we suppose that Assumptions 2.2, 2.5, 3.1, and 3.2 hold for a local primal-dual optimal solution (x_*^0, z_*^0) of the original bound-constrained problem (1.1). In what follows, (x_*^μ, z_*^μ) for $\mu \in [0, \hat{\mu}]$ denotes the primal-dual optimal solutions along the differentiable central path, as defined in Theorem 2.4. In the analysis, neighborhoods are defined in a scaled norm that takes the geometry of the barrier terms into account. For a given radius $\delta \in \mathbb{R}_{>0}$, we define the open ball

$$B_\delta(x_*^\mu) = \{x \in \mathbb{R}^n : \|x - x_*^\mu\|_{(X_*^\mu)^{-2}} < \delta\}, \quad (4.1)$$

and we denote its closure with $\bar{B}_\delta(x_*^\mu)$. Without loss of generality, we assume that $x_*^\mu = (x_{*,\mathcal{A}}^\mu, x_{*,\mathcal{I}}^\mu)$ (\mathcal{A} and \mathcal{I} defined in Assumption 2.2) and we use x_k^μ to denote the iterates generated by Algorithm 1 when it is executed for a fixed μ and define

$$G^\mu(x) = H(x) + \mu X^{-2}. \quad (4.2)$$

We let $H_k^\mu = H(x_k^\mu)$, $G_k^\mu = G(x_k^\mu)$, $H_*^\mu = H(x_*^\mu)$, and $G_*^\mu = G(x_*^\mu)$, and we use similar simplifications for the noisy quantities. We also define $z_k^\mu = \mu(X_k^\mu)^{-1}\mathbf{e}$.

This part of our analysis relies on the contraction property of Newton’s method, extended to the noisy case as analyzed in [13]. Our work goes beyond that in [13] by allowing an unbounded objective

function φ^μ and deriving constants that are independent of μ . For this analysis to be applicable, the matrix \hat{H}_k in (2.5) cannot be chosen as freely as in Section 3. Instead, we need to assume that the algorithm uses a sufficiently accurate noisy approximation of the true second derivatives $\tilde{H}_k^\mu \approx \nabla_{xx}^2 f(x_k^\mu)$ when an iterate is close to the local minimum x_*^μ . More precisely, whenever the noisy approximation of $\nabla^2 \varphi^\mu(x_k^\mu)$, given by $\tilde{G}_k^\mu := \tilde{H}_k^\mu + \mu(X_k^\mu)^{-2}$, satisfies

$$\sigma_{\min}(\tilde{G}_k^\mu) \geq \tilde{\sigma}_l^G, \quad (4.3)$$

for a fixed value $\tilde{\sigma}_l^G > 0$, the algorithm chooses $\hat{G}_k^\mu = \tilde{G}_k^\mu$ in Step 2 and computes the search direction from

$$d_k = -(\tilde{G}_k^\mu)^{-1} \nabla \tilde{\varphi}_k^\mu. \quad (4.4)$$

Lemma 4.6 guarantees the existence of a value for $\tilde{\sigma}_l^G > 0$ so that (4.3) holds when μ is sufficiently small and x_k is sufficiently close to x_*^μ , assuming that the noise $\|\tilde{H}_k^\mu - \nabla^2 f(x_k^\mu)\|$ is not too large. In this way, Assumption 2.6 remains satisfied and the convergence analysis in Section 3 still applies. At the same time, the algorithm takes steps based on a noisy Newton-type direction close to the local minimum.

We make the following standard assumption throughout this section. Recall that \mathcal{X} is defined in Assumption 3.1.

Assumption 4.1. *There exists an open set \mathcal{X}_l satisfying $\cup_{\mu \in (0, \hat{\mu}] \bar{B}_1(x_*^\mu) \subseteq \mathcal{X}_l \subseteq \mathcal{X}$ so that the Hessian $H(x)$ exists and is Lipschitz continuous over \mathcal{X} with constant $L_H \in \mathbb{R}_{>0}$, i.e., for all $x, y \in \mathcal{X}_l$, we have $\|H(x) - H(y)\| \leq L_H \|x - y\|$.*

In order to state the permissible noise level for the Hessian matrix, we define

$$\Gamma_*^0 := H_*^0 X_*^0 + Z_*^0 = \begin{pmatrix} Z_{*,\mathcal{A}}^0 & H_{*,\mathcal{A}\mathcal{I}}^0 X_{*,\mathcal{I}}^0 \\ 0 & H_{*,\mathcal{I}\mathcal{I}}^0 X_{*,\mathcal{I}}^0 \end{pmatrix}.$$

The second equality holds because $x_*^0 = (0, x_{*,\mathcal{I}}^0)$ and $z_*^0 = (z_{*,\mathcal{A}}^0, 0)$ due to complementarity. Note that this matrix is nonsingular, due to Assumption 2.2, and that

$$\lim_{\mu \rightarrow 0} G_*^\mu X_*^\mu = \lim_{\mu \rightarrow 0} (H_*^\mu X_*^\mu + Z_*^\mu) = \Gamma_*^0. \quad (4.5)$$

Assumption 4.2. *The noisy evaluation of the Hessian, denoted by \tilde{H} , satisfies*

$$\|\tilde{H}(x) - H(x)\| \leq \epsilon_H, \quad (4.6)$$

for all $x \in \mathcal{X}_l$ and some $\epsilon_H \in \mathbb{R}_{>0}$ that satisfies

$$\epsilon_H < \min \left\{ \frac{1}{4} \sigma_l^H, \frac{1}{4 \|x_*^0\|_\infty \|(\Gamma_*^0)^{-1}\|} \right\}, \quad (4.7)$$

where σ_l^H is defined in Assumption 2.2.

4.1 Local noisy quadratic-linear convergence rate

The main result of this section, stated in Theorem 4.11, is a generalization of Theorem 2.4 in [13] for the barrier problem. It is essentially a noisy version of a local quadratic convergence rate: For sufficiently small μ , there exist $M_1, M_2, M_3 \in \mathbb{R}_{>0}$ (independent of μ) so that

$$e_k^{\mu,+} \leq M_2 (e_k^\mu)^2 + M_1 \epsilon_H e_k^\mu + M_0 \epsilon_g, \quad (4.8)$$

where $e_k^\mu = \|x_k - x_*^\mu\|_{(X_*^\mu)^{-2}}$ and $e_k^{\mu,+} = \|x_k + d_k - x_*^\mu\|_{(X_*^\mu)^{-2}}$. That is, when the noise level is small compared to the error in the iterates, the steps are almost locally quadratically convergent. However, when the iterates get closer to the true optimal solution, the steps are merely linearly convergent, and eventually the noise limits how accurately the iterates can approach the optimal solution.

As in [13], we need to assume that the iterates are sufficiently close to x_*^μ for the contraction property (4.8) to hold. Most of the results in this section are valid for iterates $x_k^\mu \in \bar{B}_{\bar{\delta}}(x_*^\mu)$ where the radius $\bar{\delta}$ satisfies

$$\bar{\delta} \in \left(0, \xi_\delta \cdot \min \left\{ \frac{\sigma_l^H}{2L_H}, \frac{1}{2\tilde{L}^0 \|(\Gamma_*^0)^{-1}\|}, 1 \right\} \right], \quad (4.9)$$

with $\tilde{L}^0 = L_H \|x_*^0\|_\infty^2 + \frac{2-\bar{\delta}}{(1-\bar{\delta})^2} \|z_*^0\|_\infty$ and a fixed parameter $\xi_\delta \in (0, 1)$ arbitrarily close to one. Note that the constant \tilde{L}^0 on the right-hand side of (4.9) also depends on $\bar{\delta}$. Nevertheless, since \tilde{L}^0 converges to a positive number as $\bar{\delta} \rightarrow 0$ due to Assumption 2.2, there always exists a value of $\bar{\delta} \in (0, 1)$ that satisfies (4.9).

We begin our analysis with some technical results.

Lemma 4.3. *Let $\mu \in (0, \hat{\mu}]$ (with $\hat{\mu}$ from Theorem 2.4) and $\delta \in (0, 1)$, and suppose $x \in \bar{B}_\delta(x_*^\mu)$. Then*

$$\frac{1}{1+\delta} \leq \frac{x_{*,i}^\mu}{x_i} \leq \frac{1}{1-\delta} \quad \text{for all } i \in [n]. \quad (4.10)$$

Proof. By the definition of the $\|\cdot\|_{(X_*^\mu)^{-2}}$ -norm

$$\delta^2 \geq \|x - x_*^\mu\|_{(X_*^\mu)^{-2}}^2 = \sum_{i=1}^n \frac{|x_i - x_{*,i}^\mu|^2}{(x_{*,i}^\mu)^2},$$

which implies $\frac{|x_i - x_{*,i}^\mu|}{x_{*,i}^\mu} \leq \delta$ for all $i \in [n]$. In addition, observe that for all $i \in [n]$ $\frac{x_i}{x_{*,i}^\mu} = \frac{x_i - x_{*,i}^\mu}{x_{*,i}^\mu} + 1$. Combining the last two relationships yields (4.10). \square

Lemma 4.4. [13, Lemma 2.1] *If matrix A is non-singular and $\|A - B\| \leq \frac{1}{2\|A^{-1}\|}$, then B is non-singular, $\|B^{-1}\| < 2\|A^{-1}\|$, and $\|A^{-1} - B^{-1}\| \leq 2\|A^{-1}\|^2\|A - B\|$.*

Lemma 4.5. *There exists $\mu_1 \in (0, \hat{\mu})$ such that for all $\mu \in [0, \mu_1]$ and for all $\bar{\delta}$ satisfying (4.9), one has that*

$$\epsilon_H < \min \left\{ \frac{1}{4}\sigma_l^H, \frac{1}{4\|x_*^\mu\|_\infty \| (G_*^\mu X_*^\mu)^{-1} \|} \right\}, \quad \text{and} \quad (4.11)$$

$$\bar{\delta} \leq \min \left\{ \frac{\sigma_l^H}{2L_H}, \frac{1}{2\tilde{L}^\mu \| (G_*^\mu X_*^\mu)^{-1} \|}, 1 \right\}, \quad (4.12)$$

where $\tilde{L}^\mu = L_H \|x_*^\mu\|_\infty^2 + \frac{2-\bar{\delta}}{(1-\bar{\delta})^2} \|z_*^\mu\|_\infty$, and that, whenever $x_k^\mu \in \bar{B}_{\bar{\delta}}(x_*^\mu)$,

$$\sigma_{\min} \left(H_{k,\mathcal{I}\mathcal{I}}^\mu \right) \geq \frac{1}{4}\sigma_l^H > 0, \quad \text{and} \quad (4.13)$$

$$\sigma_{\min} \left(\tilde{H}_{k,\mathcal{I}\mathcal{I}}^\mu \right) \geq \frac{1}{4}\sigma_l^H - \epsilon_H > 0, \quad (4.14)$$

Proof. By Theorem 2.4, x_*^μ and z_*^μ are continuous functions of μ . As a consequence, all quantities on the right-hand sides of (4.11) and (4.12) depend continuously on μ and converge to the corresponding values in (4.7) and (4.9) as $\mu \rightarrow 0$. Therefore there exists $\mu_1 > 0$ so that for all $\mu \in [0, \mu_1]$ we have that (4.11) and (4.12) hold. After possibly reducing μ_1 , we further have that

$$\|x_*^\mu - x_*^0\| \leq \frac{\sigma_l^H}{2L_H}, \quad \text{for all } \mu \in [0, \mu_1]. \quad (4.15)$$

By Assumption 4.1, one has $\|H_{*,\mathcal{II}}^\mu - H_{*,\mathcal{II}}^0\| \leq L_H \|x_*^\mu - x_*^0\|$, which combined with (4.15) yields $\|H_{*,\mathcal{II}}^\mu - H_{*,\mathcal{II}}^0\| \leq \frac{\sigma_l^H}{2}$. Thus, by Lemma 4.4

$$\|(H_{*,\mathcal{II}}^\mu)^{-1}\| \leq 2\|(H_{*,\mathcal{II}}^0)^{-1}\| \leq \frac{2}{\sigma_l^H}. \quad (4.16)$$

For $x_k^\mu \in \bar{B}_{\bar{\delta}}(x_*^\mu)$, by Assumption 4.1 and (4.12) we have

$$\|H_{*,\mathcal{II}}^\mu - H_{k,\mathcal{II}}^\mu\| \leq L_H \|x_*^\mu - x_k^\mu\| = L_H e_k^\mu \leq L_H \bar{\delta} \leq \frac{\sigma_l^H}{2}.$$

Hence, applying Lemma 4.4 again, along with (4.16), yields

$$\|(H_{k,\mathcal{II}}^\mu)^{-1}\| \leq 2\|(H_{*,\mathcal{II}}^\mu)^{-1}\| \leq \frac{4}{\sigma_l^H},$$

or equivalently (4.13) holds. Finally

$$\begin{aligned} \sigma_{\min}(\tilde{H}_{k,\mathcal{II}}^\mu) &= \sigma_{\min}(H_{k,\mathcal{II}}^\mu - (H_{k,\mathcal{II}}^\mu - \tilde{H}_{k,\mathcal{II}}^\mu)) \\ &\geq \sigma_{\min}(H_{k,\mathcal{II}}^\mu) - \sigma_{\max}(H_{k,\mathcal{II}}^\mu - \tilde{H}_{k,\mathcal{II}}^\mu) \\ &= \sigma_{\min}(H_{k,\mathcal{II}}^\mu) - \|H_{k,\mathcal{II}}^\mu - \tilde{H}_{k,\mathcal{II}}^\mu\|, \end{aligned}$$

which implies (4.14) due to (4.6) and (4.11). \square

The following lemma shows that the search direction can be computed in (4.4).

Lemma 4.6. *Suppose $\bar{\delta} \in (0, 1)$ satisfies (4.9). Then, there exist $\mu_2 \in (0, \mu_1]$, and $\sigma_l^G, \tilde{\sigma}_l^G \in \mathbb{R}_{>0}$ so that for all $\mu \in [0, \mu_2]$ one has that*

$$\sigma_{\min}(G_k^\mu) \geq \sigma_l^G, \quad \text{and} \quad \sigma_{\min}(\tilde{G}_k^\mu) \geq \tilde{\sigma}_l^G,$$

whenever $x_k^\mu \in \bar{B}_{\bar{\delta}}(x_*^\mu)$. In particular, G_k^μ and \tilde{G}_k^μ are nonsingular if $x_k^\mu \in \bar{B}_{\bar{\delta}}(x_*^\mu)$.

Proof. We first prove the existence of σ_l^G . Let μ_1 be the threshold from Lemma 4.5 and let $\lambda_H = \frac{\sigma_l^H}{8}$, and $M_H = \max_{\mu \in [0, \mu_1], x \in \bar{B}_{\bar{\delta}}(x_*^\mu)} \|H(x)\|$. Define the quadratic $\phi(t) = -(\lambda_H + M_H)t^2 - 2M_H t + \lambda_H$ and let $M_A \in (0, 1)$ be its positive root.

Now suppose $x_k^\mu \in \bar{B}_{\bar{\delta}}(x_*^\mu)$ and choose any $v \in \mathbb{R}^n$ with $\|v\| = 1$. We need to show that there exists $\sigma_l^G \in \mathbb{R}_{>0}$ such that $v^T G_k^\mu v \geq \sigma_l^G$ for all sufficiently small μ independent of the particular choices of v and x_k^μ . We consider the following two cases where we set $v = (v_{\mathcal{A}}, v_{\mathcal{I}})$ with the $v_{\mathcal{A}}$ and $v_{\mathcal{I}}$ correspond to the index sets \mathcal{A} and \mathcal{I} .

Case (i): Suppose $\|v_{\mathcal{A}}\| \leq M_A$. Then $-(\lambda_H + M_H)\|v_{\mathcal{A}}\|^2 - 2M_H\|v_{\mathcal{A}}\| + \lambda_H \geq 0$, because M_A is the positive root of $\phi(t)$, $\|v_{\mathcal{A}}\|$ is between the roots, and ϕ is concave. By $1 = \|v\|^2 = \|v_{\mathcal{I}}\|^2 + \|v_{\mathcal{A}}\|^2$, one concludes that $\|v_{\mathcal{I}}\| \leq 1$. Substituting these relationships into the previous inequality yields, for any $\mu \in [0, \mu_1]$ that $0 \leq \lambda_H\|v_{\mathcal{I}}\|^2 - M_H\|v_{\mathcal{A}}\|^2 - 2M_H\|v_{\mathcal{I}}\|\|v_{\mathcal{A}}\|$. Using (4.13) and the definition of λ_H we have $\lambda_H\|v_{\mathcal{I}}\|^2 = \frac{1}{4}\sigma_l^H\|v_{\mathcal{I}}\|^2 - \frac{1}{8}\sigma_l^H\|v_{\mathcal{I}}\|^2 \leq v_{\mathcal{I}}^T H_{k,\mathcal{II}}^\mu v_{\mathcal{I}} - \frac{1}{8}\sigma_l^H\|v_{\mathcal{I}}\|^2$. Combining the last two inequalities yields

$$0 \leq -\frac{1}{8}\sigma_l^H\|v_{\mathcal{I}}\|^2 + v_{\mathcal{I}}^T H_{k,\mathcal{II}}^\mu v_{\mathcal{I}} + v_{\mathcal{A}}^T H_{k,\mathcal{AA}}^\mu v_{\mathcal{A}} + 2v_{\mathcal{I}}^T H_{k,\mathcal{IA}}^\mu v_{\mathcal{A}}, \quad (4.17)$$

where we used the definition of M_H and the fact that $\|H_{k,\mathcal{AA}}^\mu\| \leq \|H_k^\mu\|$ and $\|H_{k,\mathcal{IA}}^\mu\| \leq \|H_k^\mu\|$. Combining (4.2) with $z_k^\mu = \mu(X_k^\mu)^{-1}\mathbf{e}$ we obtain

$$v^T G_k^\mu v = v_{\mathcal{I}}^T H_{k,\mathcal{II}}^\mu v_{\mathcal{I}} + v_{\mathcal{A}}^T H_{k,\mathcal{AA}}^\mu v_{\mathcal{A}} + 2v_{\mathcal{I}}^T H_{k,\mathcal{IA}}^\mu v_{\mathcal{A}} \quad (4.18)$$

$$+ v_{\mathcal{I}}^T Z_{k,\mathcal{I}}^\mu (X_{k,\mathcal{I}}^\mu)^{-1} v_{\mathcal{I}} + v_{\mathcal{A}}^T Z_{k,\mathcal{A}}^\mu (X_{k,\mathcal{A}}^\mu)^{-1} v_{\mathcal{A}}.$$

Because the last two terms are non-negative, this together with (4.17) leaves us with $v^T G_k^\mu v \geq \frac{1}{8} \sigma_l^H \|v_{\mathcal{I}}\|^2$. Since $\|v_{\mathcal{I}}\|^2 = 1 - \|v_{\mathcal{A}}\|^2$, $\|v_{\mathcal{A}}\| \leq M_{\mathcal{A}}$, and $M_{\mathcal{A}} \in (0, 1)$, it follows that $v^T G_k^\mu v \geq \sigma_l^G$ with $\sigma_l^G = \frac{1}{8} \sigma_l^H (1 - M_{\mathcal{A}}^2) > 0$ for all $\mu \in (0, \mu_1]$.

Case (ii): Suppose that $\|v_{\mathcal{A}}\| > M_{\mathcal{A}}$. Since $\|v\| = 1$ and H_k^μ is uniformly bounded, the first three terms on the right-hand side of (4.18) are uniformly bounded below by a constant $M \in \mathbb{R}$ for all $\mu \in (0, \mu_1]$. Since the fourth term is non-negative, we obtain

$$v^T G_k^\mu v \geq M + v_{\mathcal{A}}^T Z_{k,\mathcal{A}}^\mu (X_{k,\mathcal{A}}^\mu)^{-1} v_{\mathcal{A}} \geq M + \min_{i \in \mathcal{A}} \frac{z_{k,i}^\mu}{x_{k,i}^\mu} \cdot M_{\mathcal{A}}^2 \quad (4.19)$$

for all $\mu \in (0, \mu_1]$. By $z_{k,i}^\mu = \mu/x_{k,i}^\mu$, Lemma 4.3, and $\bar{\delta} \in (0, 1)$ we have for $i \in [n]$

$$\frac{z_{k,i}^\mu}{x_{k,i}^\mu} = \frac{z_{*,i}^\mu}{x_{*,i}^\mu} \left(\frac{x_{*,i}^\mu}{x_{k,i}^\mu} \right)^2 \geq \frac{z_{*,i}^\mu}{x_{*,i}^\mu} \left(\frac{1}{1+\bar{\delta}} \right)^2 > \frac{1}{4} \frac{z_{*,i}^\mu}{x_{*,i}^\mu}.$$

By strict complementarity (Assumption 2.2) one concludes $\frac{z_{*,i}^\mu}{x_{*,i}^\mu} \rightarrow \infty$ and therefore $\frac{z_{k,i}^\mu}{x_{k,i}^\mu} \rightarrow \infty$ for all $i \in \mathcal{A}$ as $\mu \rightarrow 0$. Then (4.19) implies that there exists $\mu_2 \in (0, \mu_1]$ such that $v^T G_k^\mu v \geq \sigma_l^G$ for all $\mu \in (0, \mu_2]$.

The existence of $\tilde{\sigma}_l^G$ follows from the same arguments, after replacing H_k^μ by \tilde{H}_k^μ and $\lambda_H = \frac{\sigma_l^H}{8}$ by $\lambda_H = \frac{1}{2}(\frac{1}{4}\sigma_l^H - \epsilon_H)$. Observe that λ_H is still positive, due to (4.14). \square

We now present an iteration-dependent version of the first main result (4.8). We will make repeated use of the relationship $\|(X_*^\mu)^{-1}V\| = \sigma_{\max}((X_*^\mu)^{-1}V) = \|(X_*^\mu)^{-1}v\|_\infty \leq \|(X_*^\mu)^{-1}v\| = \|v\|_{(X_*^\mu)^{-2}}$ for $v \in \mathbb{R}_{\geq 0}^n$.

Lemma 4.7. *Let $\mu \in (0, \mu_2]$ where μ_2 is the threshold from Lemma 4.6, and suppose $\bar{\delta} \in (0, 1)$ satisfies (4.9). Then, for $x_k^\mu \in \tilde{B}_{\bar{\delta}}(x_*^\mu)$*

$$\begin{aligned} e_k^{\mu,+} &\leq M_k^{H,\mu} \|(G_k^\mu X_*^\mu)^{-1}\| (e_k^\mu)^2 \\ &\quad + M_k^{g,\mu} \|(G_k^\mu X_*^\mu)^{-1} - (\tilde{G}_k^\mu X_*^\mu)^{-1}\| e_k^\mu + \|(\tilde{G}_k^\mu X_*^\mu)^{-1}\| \epsilon_g \end{aligned} \quad (4.20)$$

with

$$M_k^{H,\mu} = \frac{L_H \|x_*^\mu\|_\infty^2}{2} + \mu \|X_*^\mu (X_k^\mu)^{-2}\| \quad \text{and} \quad M_k^{g,\mu} = L_g \|x_*^\mu\|_\infty + \mu \|(X_k^\mu)^{-1}\|.$$

Proof. Consider the noisy Newton step (4.4). Note that \tilde{G}_k^μ and G_k^μ are nonsingular due to Lemma 4.6. With $\nabla \varphi_*^\mu = 0$ this yields

$$\begin{aligned} x_k^\mu + d_k &= x_k^\mu + (\tilde{G}_k^\mu)^{-1} \nabla \tilde{\varphi}_k^\mu \\ &= x_k^\mu - (G_k^\mu)^{-1} \nabla \varphi_k^\mu \\ &\quad + \left((G_k^\mu)^{-1} - (\tilde{G}_k^\mu)^{-1} \right) (\nabla \varphi_k^\mu - \nabla \varphi_*^\mu) + (\tilde{G}_k^\mu)^{-1} (\nabla \varphi_k^\mu - \nabla \tilde{\varphi}_k^\mu) \\ &= x_k^\mu - (G_k^\mu)^{-1} (\nabla \varphi_k^\mu - \nabla \varphi_*^\mu) + \left((G_k^\mu)^{-1} - (\tilde{G}_k^\mu)^{-1} \right) (\nabla \varphi_k^\mu - \nabla \varphi_*^\mu) \\ &\quad + (\tilde{G}_k^\mu)^{-1} (g_k^\mu - \tilde{g}_k^\mu) \\ &= x_k^\mu - (G_k^\mu)^{-1} (g_k^\mu - g_*^\mu - \mu ((X_k^\mu)^{-1} - (X_*^\mu)^{-1}) \mathbf{e}) \\ &\quad + \left((G_k^\mu)^{-1} - (\tilde{G}_k^\mu)^{-1} \right) (\nabla \varphi_k^\mu - \nabla \varphi_*^\mu) + (\tilde{G}_k^\mu)^{-1} (g_k^\mu - \tilde{g}_k^\mu), \end{aligned} \quad (4.21)$$

where the third equality is obtained by the fact that $\nabla\varphi_k^\mu - \nabla\tilde{\varphi}_k^\mu = g_k^\mu - \tilde{g}_k^\mu$. In addition, by Taylor's theorem we have

$$g_k^\mu - g_*^\mu = \bar{H}_k^\mu(x_k^\mu - x_*^\mu), \quad (4.22)$$

where $\bar{H}_k^\mu := \int_0^1 \nabla^2 f(x_k^\mu + t(x_*^\mu - x_k^\mu)) dt$. Combining (4.21) and (4.22), and subtracting x_*^μ from both sides of (4.21) leads to

$$\begin{aligned} x_k^\mu + d_k - x_*^\mu &= (G_k^\mu)^{-1} (G_k^\mu - \bar{H}_k^\mu - \mu(X_k^\mu)^{-1}(X_*^\mu)^{-1}) (x_k^\mu - x_*^\mu) \\ &\quad + \left((G_k^\mu)^{-1} - (\tilde{G}_k^\mu)^{-1} \right) (\nabla\varphi_k^\mu - \nabla\varphi_*^\mu) + (\tilde{G}_k^\mu)^{-1} (g_k^\mu - \tilde{g}_k^\mu) \\ &= (G_k^\mu)^{-1} (H_k^\mu - \bar{H}_k^\mu + \mu((X_k^\mu)^{-2} - (X_k^\mu)^{-1}(X_*^\mu)^{-1})) (x_k^\mu - x_*^\mu) \\ &\quad + \left((G_k^\mu)^{-1} - (\tilde{G}_k^\mu)^{-1} \right) (\nabla\varphi_k^\mu - \nabla\varphi_*^\mu) + (\tilde{G}_k^\mu)^{-1} (g_k^\mu - \tilde{g}_k^\mu). \end{aligned}$$

Multiplying this from the left by $(X_*^\mu)^{-1}$ and rearranging terms yields

$$\begin{aligned} &(X_*^\mu)^{-1}(x_k + d_k - x_*^\mu) \\ &= (G_k^\mu X_*^\mu)^{-1} (H_k^\mu - \bar{H}_k^\mu - \mu(X_*^\mu)^{-1}(X_k^\mu)^{-2}(X_k^\mu - X_*^\mu)) (x_k^\mu - x_*^\mu) \\ &\quad + \left((G_k^\mu X_*^\mu)^{-1} - (\tilde{G}_k^\mu X_*^\mu)^{-1} \right) (g_k^\mu - g_*^\mu + \mu(X_*^\mu)^{-1}(X_k^\mu)^{-1}(x_k^\mu - x_*^\mu)) \\ &\quad + (\tilde{G}_k^\mu X_*^\mu)^{-1} (g_k^\mu - \tilde{g}_k^\mu). \end{aligned}$$

Taking norms from both sides along with Assumptions 2.5, 3.1, and 4.1 implies

$$\begin{aligned} &\|x_k^\mu + d_k - x_*^\mu\|_{(X_*^\mu)^{-2}} \\ &\leq \|(G_k^\mu X_*^\mu)^{-1}\| \|(H_k^\mu - \bar{H}_k^\mu - \mu X_*^\mu (X_k^\mu)^{-2} (X_k^\mu - X_*^\mu) (X_*^\mu)^{-2}) (x_k^\mu - x_*^\mu)\| \\ &\quad + \|(G_k^\mu X_*^\mu)^{-1} - (\tilde{G}_k^\mu X_*^\mu)^{-1}\| \|g_k^\mu - g_*^\mu + \mu(X_*^\mu)^{-1}(X_k^\mu)^{-1}(x_k^\mu - x_*^\mu)\| \\ &\quad + \|(\tilde{G}_k^\mu X_*^\mu)^{-1}\| \|g_k^\mu - \tilde{g}_k^\mu\| \\ &\leq \|(G_k^\mu X_*^\mu)^{-1}\| \left(\frac{L_H \|X_*^\mu\|^2}{2} + \mu \|X_*^\mu (X_k^\mu)^{-2}\| \right) \|x_k^\mu - x_*^\mu\|_{(X_*^\mu)^{-2}}^2 \\ &\quad + \|(G_k^\mu X_*^\mu)^{-1} - (\tilde{G}_k^\mu X_*^\mu)^{-1}\| (L_g \|X_*^\mu\| + \mu \|(X_k^\mu)^{-1}\|) \|x_k^\mu - x_*^\mu\|_{(X_*^\mu)^{-2}} \\ &\quad + \|(\tilde{G}_k^\mu X_*^\mu)^{-1}\| \epsilon_g. \end{aligned}$$

This completes the proof. \square

Our next goal is to establish upper bounds for all the terms on the right-hand side of (4.20). We accomplish this with the following lemmas.

Lemma 4.8. *Let $\mu \in (0, \mu_2]$ with μ_2 from Lemma 4.6, and suppose $\bar{\delta} \in (0, 1)$ satisfies (4.9). Then for $x_k^\mu \in \bar{B}_{\bar{\delta}}(x_*^\mu)$, $\|G_k^\mu X_*^\mu - G_*^\mu X_*^\mu\| \leq \frac{1}{2\|(G_*^\mu X_*^\mu)^{-1}\|}$.*

Proof. By the definition of G_k^μ and G_*^μ , and Assumption 4.1 we have

$$\begin{aligned} &\|G_k^\mu X_*^\mu - G_*^\mu X_*^\mu\| \\ &\leq \|(H_k^\mu - H_*^\mu)X_*^\mu + \mu((X_k^\mu)^{-2} - \mu(X_*^\mu)^{-2})X_*^\mu\| \\ &\leq L_H \|X_*^\mu\|^2 \|x_k^\mu - x_*^\mu\|_{(X_*^\mu)^{-2}} + \mu \|(X_*^\mu)^{-2}(X_k^\mu)^{-2}((X_*^\mu)^2 - (X_k^\mu)^2)X_*^\mu\| \\ &\leq L_H \|x_*^\mu\|_\infty^2 \|x_k^\mu - x_*^\mu\|_{(X_*^\mu)^{-2}} \end{aligned}$$

$$\begin{aligned}
& + \mu \|(X_*^\mu)^{-2}(X_k^\mu)^{-2}(X_*^\mu + X_k^\mu)(X_*^\mu)^2\| \|x_k^\mu - x_*^\mu\|_{(X_*^\mu)^{-2}} \\
& = (L_H \|x_*^\mu\|_\infty^2 + \mu \|(X_*^\mu)^{-1}(X_*^\mu(X_k^\mu)^{-1})(I + X_*^\mu(X_k^\mu)^{-1})\|) \|x_k^\mu - x_*^\mu\|_{(X_*^\mu)^{-2}} \\
& \leq (L_H \|x_*^\mu\|_\infty^2 + \mu \|(X_*^\mu)^{-1}\| \|X_*^\mu(X_k^\mu)^{-1}\| (1 + \|X_*^\mu(X_k^\mu)^{-1}\|)) \|x_k^\mu - x_*^\mu\|_{(X_*^\mu)^{-2}}.
\end{aligned}$$

Since $\|x_k^\mu - x_*^\mu\|_{(X_*^\mu)^{-2}} \leq \bar{\delta}$ ($\bar{\delta}$ satisfies (4.12)), Lemma 4.3 and $z_*^\mu = \mu(X_*^\mu)^{-1}\mathbf{e}$ yield

$$\begin{aligned}
\|G_k^\mu X_*^\mu - G_*^\mu X_*^\mu\| & \leq \left(L_H \|x_*^\mu\|_\infty^2 + \frac{\|z_*^\mu\|_\infty}{1-\bar{\delta}} \left(1 + \frac{1}{1-\bar{\delta}} \right) \right) \|x_k^\mu - x_*^\mu\|_{(X_*^\mu)^{-2}} \\
& = \tilde{L}^\mu \|x_k^\mu - x_*^\mu\|_{(X_*^\mu)^{-2}} \leq \frac{1}{2\|(G_*^\mu X_*^\mu)^{-1}\|}.
\end{aligned}$$

□

Lemma 4.9. *Let μ_2 be the threshold from Lemma 4.6 and suppose $\bar{\delta} \in (0, 1)$ satisfies (4.9). Then, there exists $\mu_3 \in (0, \mu_2]$ so that for all $x_k^\mu \in \bar{B}_{\bar{\delta}}(x_*^\mu)$ one has*

$$\|(G_k^\mu X_*^\mu)^{-1}\| \leq 4 \|(\Gamma_*^0)^{-1}\|.$$

Proof. By Assumptions 3.1 and 4.1 and $\mu(X_*^\mu)^{-1} = Z_*^\mu$ one has for all $\mu \in (0, \mu_2]$

$$\begin{aligned}
\|G_*^\mu X_*^\mu - \Gamma_*^0\| & = \|H_*^\mu X_*^\mu + \mu(X_*^\mu)^{-1} - (H_*^0 X_*^0 + Z_*^0)\| \\
& = \|H_*^\mu X_*^\mu - H_*^\mu X_*^0 + H_*^\mu X_*^0 - H_*^0 X_*^0 + Z_*^\mu - Z_*^0\| \\
& \leq \|H_*^\mu\| \|x_*^\mu - x_*^0\| + L_H \|x_*^0\|_\infty \|x_*^\mu - x_*^0\| + \|z_*^\mu - z_*^0\| \\
& \leq \max\{L_g + L_H \|x_*^0\|_\infty, 1\} (\|x_*^\mu - x_*^0\| + \|z_*^\mu - z_*^0\|),
\end{aligned} \tag{4.23}$$

and by continuity of (x_*^μ, z_*^μ) as a function of μ

$$\|x_*^\mu - x_*^0\| + \|z_*^\mu - z_*^0\| \leq \frac{1}{2\max\{L_g + L_H \|x_*^0\|_\infty, 1\} \|(\Gamma_*^0)^{-1}\|}, \tag{4.24}$$

for all $\mu \in (0, \mu_3]$ with $\mu_3 \in (0, \mu_2]$ sufficiently small. Fixing $\mu \in (0, \mu_3]$ and combining (4.23) and (4.24) yields $\|G_*^\mu X_*^\mu - \Gamma_*^0\| \leq \frac{1}{2\|(\Gamma_*^0)^{-1}\|}$. By Lemma 4.4 one has

$$\|(G_*^\mu X_*^\mu)^{-1}\| \leq 2 \|(\Gamma_*^0)^{-1}\|. \tag{4.25}$$

By Lemma 4.8, we have $\|G_k^\mu X_*^\mu - G_*^\mu X_*^\mu\| \leq \frac{1}{2\|(G_*^\mu X_*^\mu)^{-1}\|}$. This, along with Lemma 4.4 implies $\|(G_k^\mu X_*^\mu)^{-1}\| \leq 2\|(G_*^\mu X_*^\mu)^{-1}\|$ and by (4.25) the desired result follows. □

Lemma 4.10. *Let $\mu \in (0, \mu_3]$ where μ_3 is the threshold from Lemma 4.9, and suppose $\bar{\delta} \in (0, 1)$ satisfies (4.9). Then for $x_k^\mu \in \bar{B}_{\bar{\delta}}(x_*^\mu)$*

$$\begin{aligned}
\|(G_k^\mu X_*^\mu)^{-1} - (\tilde{G}_k^\mu X_*^\mu)^{-1}\| & \leq 2\|(G_k^\mu X_*^\mu)^{-1}\|^2 \|x_*^\mu\|_\infty \epsilon_H, \\
\|(\tilde{G}_k^\mu X_*^\mu)^{-1}\| & \leq 2\|(G_k^\mu X_*^\mu)^{-1}\|.
\end{aligned}$$

Proof. By Lemmas 4.4 and 4.8, one concludes that $\|(G_k^\mu X_*^\mu)^{-1}\| \leq 2\|(G_*^\mu X_*^\mu)^{-1}\|$. Hence, by (4.11) we obtain

$$\begin{aligned}
\|G_k^\mu X_*^\mu - \tilde{G}_k^\mu X_*^\mu\| & = \|H_k^\mu - \tilde{H}_k^\mu\| \|X_*^\mu\| \leq \|x_*^\mu\|_\infty \epsilon_H \\
& \leq \frac{1}{4\|(G_*^\mu X_*^\mu)^{-1}\|} \leq \frac{1}{2\|(G_k^\mu X_*^\mu)^{-1}\|},
\end{aligned}$$

and by Lemma 4.4, we get the desired results. □

Theorem 4.11. *Let μ_3 be the threshold from Lemma 4.9 and suppose $\bar{\delta} \in (0, 1)$ satisfies (4.9). Furthermore, let $\xi_M \in (1, \infty)$ and define*

$$\begin{aligned} M_2 &= \xi_M \cdot 4 \|(\Gamma_*^0)^{-1}\| \left(\frac{L_H \|x_*^0\|_\infty^2}{2} + \frac{\|z_*^0\|_\infty}{(1-\bar{\delta})^2} \right), \\ M_1 &= \xi_M \cdot 32 \|(\Gamma_*^0)^{-1}\|^2 \|x_*^0\|_\infty \left(L_g \|x_*^0\|_\infty + \frac{\|z_*^0\|_\infty}{1-\bar{\delta}} \right), \\ M_0 &= 8 \|(\Gamma_*^0)^{-1}\|. \end{aligned} \quad (4.26)$$

Then there exists $\bar{\mu} \in (0, \mu_3]$ so that for all $\mu \in (0, \bar{\mu}]$

$$e_k^{\mu,+} \leq M_2 (e_k^\mu)^2 + M_1 \epsilon_H e_k^\mu + M_0 \epsilon_g, \quad (4.27)$$

whenever $x_k^\mu \in \bar{B}_{\bar{\delta}}(x_*)$.

Proof. By Lemmas 4.7 and 4.10 one has

$$e_k^+ \leq M_k^{H,\mu} \| (G_k^\mu X_*^\mu)^{-1} \| (e_k^\mu)^2 + 2M_k^{g,\mu} \| (G_k^\mu X_*^\mu)^{-1} \|^2 \|x_*^\mu\|_\infty \epsilon_H e_k^\mu + 2 \| (G_k^\mu X_*^\mu)^{-1} \| \epsilon_g.$$

Lemmas 4.3 and 4.9, together with (4.11) and (4.12), imply that (4.27) holds with

$$\begin{aligned} M_2^0 &= 4 \|(\Gamma_*^0)^{-1}\| \left(\frac{L_H \|x_*^\mu\|_\infty^2}{2} + \frac{\|z_*^\mu\|_\infty}{(1-\bar{\delta})^2} \right), \\ M_1^0 &= 32 \|(\Gamma_*^0)^{-1}\|^2 \|x_*^\mu\|_\infty \left(L_g \|x_*^\mu\|_\infty + \frac{\|z_*^\mu\|_\infty}{1-\bar{\delta}} \right), \\ M_0^0 &= 8 \|(\Gamma_*^0)^{-1}\|. \end{aligned}$$

Since x_*^μ and z_*^μ are continuous due to Theorem 2.4 and since $\xi_M > 1$, there exists $\bar{\mu} \in (0, \mu_3]$ so that (4.27) holds for all $\mu \in (0, \bar{\mu}]$ with the constants defined in (4.26). \square

4.2 Convergence into neighborhoods around the optimal solution

We first prove a uniform lower bound on the step size, to ensure sufficient progress is made in every iteration.

Lemma 4.12. *Let $\mu > 0$. Then there exists $\bar{\alpha}^\mu > 0$, such that $\alpha_k \geq \bar{\alpha}^\mu/2$ for all $k \in \mathbb{N}$, where α_k is step size sequence generated in Steps 4–6 when Algorithm 1 is executed for fixed μ .*

Proof. Let $k \in \mathbb{N}$. As in the proof of Lemma 3.6 we can derive (3.3) where $\check{G}_k^\mu = \check{H}_k^\mu + \frac{2\mu}{1-\tau} (X_k^\mu)^{-2}$. Then, using Assumption 2.5, (3.3), and Lemma 3.4, we have

$$\begin{aligned} & \tilde{\varphi}^\mu(x_k^\mu + \alpha_k d_k) - \tilde{\varphi}^\mu(x_k^\mu) - \nu \alpha_k (\nabla \tilde{\varphi}_k^\mu)^T d_k - \epsilon_R \\ & \leq \varphi^\mu(x_k^\mu + \alpha_k d_k) - \varphi^\mu(x_k^\mu) - \nu \alpha_k (\nabla \varphi_k^\mu)^T d_k + \nu \alpha_k \|d_k\| \epsilon_g + 2\epsilon_f - \epsilon_R \\ & \leq (1-\nu) \alpha_k (\nabla \varphi_k^\mu)^T d_k + \frac{\alpha_k^2}{2} d_k^T \check{G}_k^\mu d_k + \nu \alpha_k \|d_k\| \epsilon_g + 2\epsilon_f - \epsilon_R \\ & \leq (1-\nu) \alpha_k \|\nabla \varphi_k^\mu\| \|d_k\| + \frac{\alpha_k^2}{2} \left(L_g + \frac{2\mu}{(1-\tau)\delta_x^2} \right) \|d_k\|^2 + \nu \alpha_k \|d_k\| \epsilon_g + 2\epsilon_f - \epsilon_R. \end{aligned} \quad (4.28)$$

To examine the right-hand side, we define the convex quadratic function $\phi(\alpha) = a\alpha^2 + b\alpha - c$ with

$$\begin{aligned} a &:= \frac{1}{2} \left(L_g + \frac{2\mu}{(1-\tau)\delta_x^2} \right) \|d_k\|^2 > 0, \\ b &:= ((1-\nu) \|\nabla \varphi_k^\mu\| + \nu \epsilon_g) \|d_k\| > 0, \end{aligned}$$

$$c := \epsilon_R - 2\epsilon_f > 0,$$

and let $\bar{\alpha}_k > 0$ be the positive root of $\phi(\alpha)$. Then by (4.28), the Armijo condition (2.8) is satisfied when $\phi(\alpha_k) \leq 0$, which is the case when $\alpha_k \in (0, \bar{\alpha}_k]$. From Steps 4–6 we can then conclude that $\alpha_k \geq \bar{\alpha}_k/2$. Because a and b are uniformly bounded by Lemmas 3.4 and 3.5 for all k , $\bar{\alpha}_k$ is uniformly bounded away from 0 (see Lemma B.1 in Appendix B). It follows that $\alpha_k \geq \inf_{k' \in \mathbb{N}} \bar{\alpha}_{k'} =: \bar{\alpha}^\mu > 0$. \square

We are now ready to state the main theorem of this section.

Theorem 4.13. *Let $\bar{\mu}$ be the threshold from Lemma 4.9, and suppose $\bar{\delta} \in (0, 1)$ satisfies (4.9). Further suppose that ϵ_g and ϵ_H , in addition to (4.7), satisfy*

$$\epsilon_H < \frac{1}{M_1}, \quad \text{and} \quad \epsilon_g \leq \frac{(1 - M_1 \epsilon_H)^2}{4M_0 M_2}, \quad (4.29)$$

where M_0 , M_1 , and M_2 are defined in (4.26) (and depend on $\bar{\delta}$). Further, let

$$\delta^+, \delta^- = \frac{(1 - M_1 \epsilon_H) \pm \sqrt{\Delta}}{2M_2}, \quad \text{with} \quad \Delta = (1 - M_1 \epsilon_H)^2 - 4M_0 M_2 \epsilon_g, \quad (4.30)$$

and $\delta_1 = \delta^-$ and $\delta_2 = \min\{\delta^+, \bar{\delta}\}$ and assume $\delta_1 \leq \bar{\delta}$. Then, for all $\mu \in (0, \bar{\mu})$,

- (i) $x_k^\mu \in B_{\delta_2}(x_*^\mu) \setminus \bar{B}_{\delta_1}(x_*^\mu)$ implies $\|x_{k+1}^\mu - x_*^\mu\|_{(X_*^\mu)^{-2}} < \|x_k^\mu - x_*^\mu\|_{(X_*^\mu)^{-2}}$;
- (ii) $x_k^\mu \in \bar{B}_{\delta_1}(x_*^\mu)$ implies $x_{k+1}^\mu \in \bar{B}_{\delta_1}(x_*^\mu)$; and
- (iii) $\limsup_{k \rightarrow \infty} \|x_k^\mu - x_*^\mu\|_{(X_*^\mu)^{-2}} \leq \delta_1$.

Proof. Let $\mu \in (0, \mu_3]$ and let $\phi(e) = M_2 \cdot e^2 + M_1 \epsilon_H \cdot e + M_0 \epsilon_g$. The assumptions on ϵ_g and ϵ_H imply $\Delta, \delta^-, \delta^+ > 0$. If $x_k^\mu \in B_{\delta_2}(x_*^\mu)$, then $e_k^\mu \leq \delta_2 \leq \bar{\delta}$ and Theorem 4.11 implies $e_k^{\mu,+} \leq \phi(e_k^\mu)$. Hence

$$\begin{aligned} e_{k+1}^\mu &= \|x_{k+1}^\mu - x_*^\mu\|_{(X_*^\mu)^{-2}} = \|x_k^\mu + \alpha_k d_k - x_*^\mu\|_{(X_*^\mu)^{-2}} \\ &= \|(1 - \alpha_k)(x_k^\mu - x_*^\mu) + \alpha_k(x_k^\mu + d_k - x_*^\mu)\|_{(X_*^\mu)^{-2}} \\ &\leq (1 - \alpha_k)e_k^\mu + \alpha_k e_k^{\mu,+} \leq e_k^\mu + \alpha_k(\phi(e_k^\mu) - e_k^\mu). \end{aligned} \quad (4.31)$$

Since δ^- and δ^+ are the roots of $\psi(\delta) = \phi(\delta) - \delta$ and ψ is a strictly convex quadratic function, we have that $\psi(e_k^\mu) < 0$ when $\delta^- < e_k^\mu < \min\{\delta^+, \bar{\delta}\} = \delta_2$, and consequently $\phi(e_k^\mu) = \psi(e_k^\mu) + e_k^\mu < e_k^\mu$. Since $\alpha_k > 0$, (4.31) yields claim (i).

To show claim (ii), we first prove that $M_0 \epsilon_g \leq \delta_1 = \delta^-$. By the definition of δ^- in (4.30), this is equivalent to showing $(1 - M_1 \epsilon_H) - 2M_0 M_2 \epsilon_g \geq \sqrt{\Delta}$. Observe that $(1 - M_1 \epsilon_H) - 2M_0 M_2 \epsilon_g$ is non-negative since $\epsilon_g \leq \frac{(1 - M_1 \epsilon_H)^2}{4M_0 M_2} \leq \frac{1 - M_1 \epsilon_H}{2M_0 M_2}$ by (4.29) and $(1 - M_1 \epsilon_H) \in (0, 1)$. Thus, it is sufficient to show $((1 - M_1 \epsilon_H) - 2M_0 M_2 \epsilon_g)^2 \geq \Delta$. Expanding the quadratic on the left-hand side of this inequality and by the definition of Δ in (4.30), one has that this inequality trivially holds, as $M_0 M_2 \epsilon_g + M_1 \epsilon_H \geq 0$.

Now consider $x_k^\mu \in \bar{B}_{\delta_1}(x_*^\mu)$. Because $e_k \in [0, \delta_1]$, we have $\phi(e_k^\mu) \leq \phi(0) = M_0 \epsilon_g \leq \delta_1$ since ϕ is monotonically decreasing over $[0, \delta^-] = [0, \delta_1]$ (recall $\delta_1 = \delta^-$ by definition). Together with (4.31), this concludes the proof of claim (ii).

Finally, claim (iii) follows from part (ii) if $x_{k'} \in \bar{B}_{\delta_1}(x_*^\mu)$ for some k' . For the other case, suppose $e_{k'} > \delta_1$ for all k' and let $x_k \in B_{\delta_2}(x_*^\mu)$. Part (i) then yields that $e_{k'+1} < e_{k'}$ for all $k' \geq k$. Choose an arbitrary $\eta \in (0, -\psi(e_k))$ and recall that $\delta_1 = \delta^-$ and $\psi(e_k) < 0$ since $e_k \in (\delta^-, \delta^+)$. Let δ_η^- and

δ_η^+ be the roots of $\psi(\delta) + \eta = 0$. Then $\psi(\delta) + \eta < 0$ for all $\delta \in (\delta_\eta^-, \delta_\eta^+)$. Consequently, as long as $e_k^\mu > \delta_\eta^-$, we have $\phi(e_k^\mu) = \psi(e_k^\mu) + e_k^\mu < e_k^\mu - \eta$. Substituting this into (4.31), we have

$$e_{k+1} < (1 - \alpha_k)e_k^\mu + \alpha_k(e_k^\mu - \eta) = e_k^\mu - \alpha_k\eta \leq e_k^\mu - \bar{\alpha}^\mu\eta,$$

where $\bar{\alpha}^\mu > 0$ is the constant defined in Lemma 4.12. This shows that the error is decreased by at least $\bar{\alpha}^\mu\eta$ in each iteration as long as $e_k > \delta_\eta^-$. This, combined with the fact that $e_{k'+1} < e_{k'}$ for all $k' \geq k$, yields that $e_{k'} \leq \delta_\eta^-$ for all k' sufficiently large. To finish the proof note that the conclusion above holds for any $\eta \in (0, -\psi(e_k))$, and since $\delta_\eta^- \rightarrow \delta^-$ as $\eta \rightarrow 0$, we obtain the desired result. \square

Remark 4.14. The interpretation of this result is that, if the noise levels are sufficiently small, there exists a neighborhood $B_{\delta_1}(x_*^\mu)$ around the solution from which the iterates cannot escape once they are inside. Further, there is a larger neighborhood of attraction, $B_{\delta_2}(x_*^\mu)$, with the property that once iterates fall into this neighborhood, they converge monotonically towards $B_{\delta_1}(x_*^\mu)$ or enter $B_{\delta_1}(x_*^\mu)$. The condition on ϵ_g in (4.29) shows a trade-off between the permissible noise in the gradient and the Hessian, where ϵ_g needs to be decreased if ϵ_H increases (see Figure 3 below).

Remark 4.15. Theorem 4.13 is valid for an entire range of $\bar{\delta}$. Notice that M_0 , M_1 , and M_2 and consequently δ_1 and δ_2 depend on $\bar{\delta}$. Therefore, we can derive the largest “attraction-neighborhood” $\bar{B}_{\delta_2^{\max}}(x_*^\mu)$ from Theorem 4.13 by looking for the largest value δ_2^{\max} of δ_2 among those for which $\bar{\delta}$ satisfies the assumptions of the theorem. Similarly, defining δ_1^{\min} as the smallest possible value of δ_1 , we can find the smallest “containment-neighborhood” $\bar{B}_{\delta_1^{\min}}(x_*^\mu)$. We discuss an example of this in Section 4.3.

The following is the key observation of this section.

Remark 4.16 (Active-set identification). In the non-noisy case ($\epsilon_f = \epsilon_g = \epsilon_H = 0$), the interior-point framework obtains a solution of the original problem (1.1) by approximately solving barrier problems (2.1) for a decreasing sequence $\{\mu_\ell\}$ of barrier parameters with $\mu_\ell \rightarrow 0$. Then, for $i \in \mathcal{A}$, the iterates $x_{k,i}^{\mu_\ell}$ converge to zero when $\mu_\ell \rightarrow 0$ and Algorithm 1 is executed for sufficiently many iterations for each fixed value of μ_ℓ . In other words, the interior-point method is able to identify which bounds are active at the optimal solution. One may suspect that this is not the case when $\epsilon_f, \epsilon_g, \epsilon_H > 0$ because the iterates $x_{k,i}^{\mu_\ell}$ might keep changing significantly even for small μ_ℓ because of the noise. However, if for every μ_ℓ , for which Algorithm 1 is executed, eventually $x_k^{\mu_\ell} \in B_{\delta_2}(x_*^{\mu_\ell})$ for a sufficiently large k , then $\frac{|x_{k,i}^{\mu_\ell} - x_{*,i}^{\mu_\ell}|}{x_{*,i}^{\mu_\ell}} \leq \|(X_*^{\mu_\ell})^{-1}(x_k^{\mu_\ell} - x_*^{\mu_\ell})\| = \|x_k^{\mu_\ell} - x_*^{\mu_\ell}\|_{(X_*^{\mu_\ell})^{-2}} < \delta_2$, or equivalently $|x_{k,i}^{\mu_\ell} - x_{*,i}^{\mu_\ell}| < \delta_2 x_{*,i}^{\mu_\ell}$ for all $i \in \mathcal{A}$ and all large k . Since $\lim_{\mu \rightarrow 0} x_{*,i}^\mu = 0$ this implies that, as in the non-noisy case, $x_{k,i}^{\mu_\ell}$ converge to zero when $\mu_\ell \rightarrow 0$. In other words, the algorithm is able to identify the set of active constraints even in the presence of noise; see also Figure 2.

4.3 Illustrative example

To illustrate the implications of Remark 4.15, consider the optimization problem

$$\min_{x \in \mathbb{R}^n} \frac{1}{2} (x_1 - 1)^2 + x_2 \quad \text{s.t.} \quad x \geq 0.$$

The primal-dual path, in terms of $\mu \in [0, 1]$, is $x_*^\mu = \left(\frac{1+\sqrt{1+4\mu}}{2}, \mu\right)^T$ and $z_*^\mu = \left(\frac{2\mu}{1+\sqrt{1+4\mu}}, 1\right)^T$.

Observe that $\|z_*^\mu\|_\infty = 1$. In addition, $g(x) = (x_1 - 1, 1)^T$ and $H(x) = \begin{bmatrix} 1 & 0 \\ 0 & 0 \end{bmatrix}$ yield $L_g = 1$ and

$L_H = 0$, respectively. Also,

$$G_k^\mu X_*^\mu = \begin{bmatrix} \left(1 + \frac{\mu}{(x_{k,1}^\mu)^2}\right) x_{*,1}^\mu & 0 \\ 0 & \frac{\mu}{(x_{k,2}^\mu)^2} x_{*,2}^\mu \end{bmatrix}, \text{ and}$$

$$\|(G_k^\mu X_*^\mu)^{-1}\| = \max \left\{ \left(x_{*,1}^\mu + \frac{\mu}{x_{*,1}^\mu} \left(\frac{x_{*,1}^\mu}{x_{k,1}^\mu} \right)^2 \right)^{-1}, \frac{x_{*,2}^\mu}{\mu} \left(\frac{x_{k,2}^\mu}{x_{*,2}^\mu} \right)^2 \right\}.$$

Since $x_{*,1}^\mu > 1$, the first term in the max-term is less than 1. Also, by Lemma 4.3, one has that $(x_{k,2}^\mu/x_{*,2}^\mu)^2 \leq (1 + e_k^\mu)^2$. This, along with $\frac{x_{*,2}^\mu}{\mu} = 1$, implies that $\|(G_k^\mu X_*^\mu)^{-1}\| \leq (1 + e_k^\mu)^2 \leq (1 + \bar{\delta})^2$. Replacing $4\|(\Gamma_*^0)^{-1}\|$ with $\|(G_k^\mu X_*^\mu)^{-1}\|$ in (4.26) yields a tighter bound on e_k^+ and the constants M_2 , M_1 , and M_0 for this example are

$$M_2 = \left(\frac{1+\bar{\delta}}{1-\bar{\delta}} \right)^2, \quad M_1 = 2(1 + \bar{\delta})^4 \left(\frac{1+\sqrt{1+4\mu}}{2} \right) \left(\left(\frac{1+\sqrt{1+4\mu}}{2} \right) + \frac{1}{1-\bar{\delta}} \right), \quad M_0 = 2(1 + \bar{\delta})^2.$$

Now consider $\epsilon_g = 0.02$ and $\epsilon_H = 0.01$ with $\mu = 10^{-6}$. Figure 1 shows δ^- and δ^+ as functions of $\bar{\delta}$. For visualization purposes, we also include a plot of the *identity line* (with a slope of one), denoted by $\bar{\delta}$ in the figure legend. Note that δ^- and δ^+ are monotonically increasing and decreasing, respectively, as $\bar{\delta}$ increases. Consequently, the radii in Remark 4.15 are $\delta_1^{\min} \approx 0.05$ and $\delta_2^{\max} \approx 0.24$, computed as the roots of $\delta^- = \bar{\delta}$ and $\delta^+ = \bar{\delta}$, respectively.

Figure 2 shows the neighborhood $\bar{B}_{\delta_2^{\max}}(x_*^\mu)$ in the (x_1, x_2) -space and is a visualization for Remark 4.16. Observe that the neighborhood is much narrower in the x_2 - than in the x_1 -direction. In addition, as μ decreases the neighborhood becomes even narrower in the x_2 -direction. This implies that late iterates $x_{k,2}^\mu$ remain closer to $x_{*,2}^0 = 0$ as μ decreases despite the presence of noise in evaluating the objective function and its gradient. This observation suggests that decreasing the barrier parameter μ beyond some potential noise-induced threshold is beneficial in obtaining a more accurate solution and identifying the active constraints. In Table 2 below we see that this is observed also when the algorithm is applied to general problem instances.

Finally, we want to show that Theorem 4.13 applies to a wide range of noise thresholds ϵ_H and ϵ_g . Figure 3 depicts a plot of δ_1^{\min} and δ_2^{\max} as a function of ϵ_g and ϵ_H for $\mu = 10^{-6}$. The domain in Figure 3a and 3b corresponds to the pairs (ϵ_g, ϵ_H) for which the assumptions of Theorem 4.13 are satisfied, i.e., $\Delta \geq 0$ in (4.30). As discussed in Remark 4.14, (4.29) indicates a trade-off in the permissible values of ϵ_H and ϵ_g : When ϵ_g is large, ϵ_H needs to be small, and vice versa. Also, observe that δ_2^{\max} increases and δ_1^{\min} decreases as ϵ_g and ϵ_H decrease. In particular, $\epsilon_g = \epsilon_H = 0$ yields $\delta_1^{\min} = 0$, i.e., $\bar{B}_{\delta_1^{\min}}(x_*^\mu) = \{x_*^\mu\}$, which implies that $x_k^\mu \rightarrow x_*^\mu$ as $k \rightarrow \infty$ by part (iii) in Theorem 4.11, as one expects in the non-noisy case.

5 Numerical experiments

In this section, we present numerical results that show that the theoretical findings in Sections 3 and 4 can be observed in practice.

We performed the experiments in Matlab 2020b with a primal-dual implementation of Algorithm 1 with $\nu = 10^{-6}$ and $\epsilon_R = 2.05\epsilon_f$. The primal-dual Hessian, based on (3.1), is used in computing the search direction (2.6). Algorithm 2 in Appendix E is a formal description of the implemented method. We use the primal-dual variant because, as is well known, it significantly outperforms the primal method in terms of the number of iterations needed to converge in the non-noisy case. In

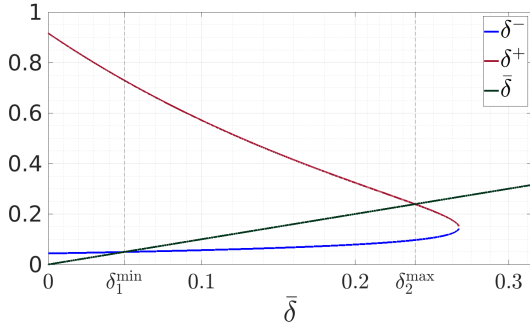


Figure 1: δ^- and δ^+ as a function of $\bar{\delta}$.

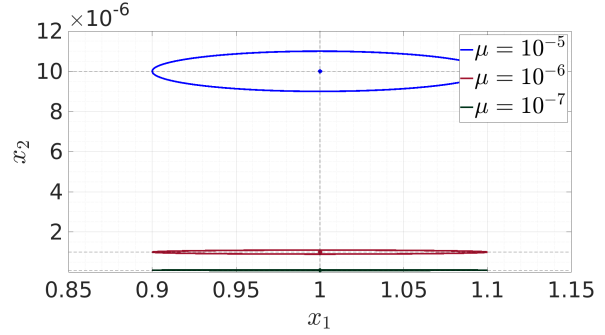


Figure 2: Illustration of $\bar{B}_{\delta_2}(x_*^\mu)$.

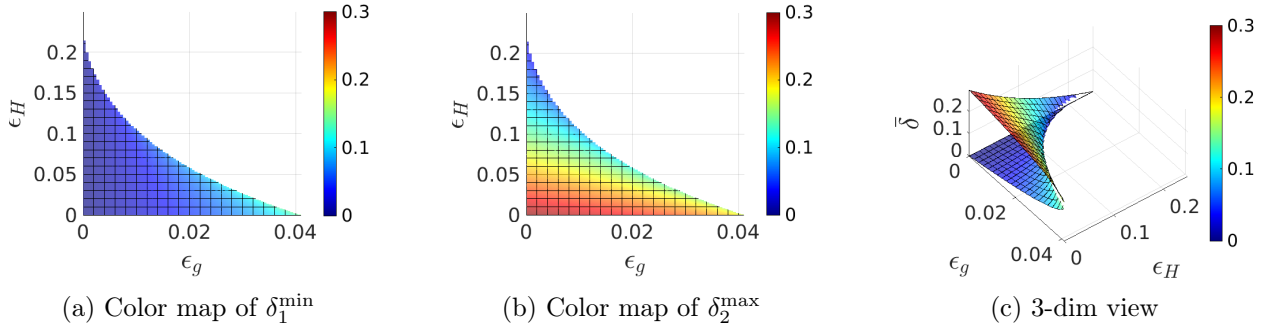


Figure 3: Dependence of δ_1^{\min} and δ_2^{\max} as a function of ϵ_g and ϵ_H .

preliminary tests, we observed the same advantage in the presence of noise. As discussed in Section 3, the global convergence results still hold for this variant.

To handle nonconvexity, we follow an approach similar to that in [17] and choose $\hat{G}_k^\mu = \hat{H}_k^\mu + Z_k^\mu (X_k^\mu)^{-1} + \lambda I$ for some $\lambda \geq 0$ to make sure that the positive-definite condition (2.9) holds. We observed in our experiments that for small values of μ , the regularization eventually chooses $\lambda = 0$ also for nonconvex instances, providing evidence for our theoretical result in Lemma 4.6.

The problems considered in this section are selected from the CUTE (Constrained and Unconstrained Testing Environment) problem collection [5]. We chose the bound-constrained instances for which the AMPL models are available [24]¹. We omitted problems in which no constraint was active at the optimal solution, as they are not relevant to verifying the theoretical results of identifying active constraints in Section 4. The sizes of the problems vary between $n = 2$ and $n = 1000$ variables.

In all experiments, we added Bernoulli-distributed noise with parameter 0.5 and magnitude ϵ_f to the deterministic objective function, and the added noise in the gradient is uniformly distributed on the surface of an n -dimensional ball with radius ϵ_g around the deterministic gradient. We further perturb the diagonal elements of the Hessian with a Bernoulli-distributed noise with parameter 0.5 and magnitude ϵ_H .

5.1 Termination test

We begin by studying the effectiveness of the stopping test in Theorem 3.9. We ran the algorithm for 1000 iterations and recorded the first iteration $k = \text{ter}$ in which condition (i) or (ii) in Theorem 3.9 holds. The results are given in Table 1, for $\mu = 10^{-1}$ and noise levels $\epsilon_f = 10^{-2}$ and $\epsilon_g = \epsilon_H = 10^{-1}$.

¹We divided the objective functions in problems `ncvxbqp*` by n .

(We choose the derivative noise ϵ_g and ϵ_H as $\sqrt{\epsilon_f}$ to imitate the errors one might obtain if the derivatives are approximated by finite differences using noisy function values.)

First, we note that the algorithm is able to solve all instances. The termination test is triggered often within a number of iterations that is very close to the iteration count for a noise-less version of the instance (solved to a tight tolerance of 10^{-6}). This indicates that the termination test is capable of detecting when the algorithm enters a regime in which steps start to be dominated by noise. Furthermore, by comparing the number of iterations with the number of function evaluations, we see that in almost all instances the first trial step size ($\alpha_k = \alpha_k^{\max}$) is accepted in the first `ter` iterations.

Comparing the unscaled optimality measures $\|\nabla\tilde{\varphi}_0^\mu\|$ and $\|\nabla\tilde{\varphi}_{\text{ter}}^\mu\|$, we see that the method made significant progress from the starting points until the termination tests were satisfied. The column $\|\nabla\tilde{\varphi}^\mu\|^{\text{av}}$ gives an idea of the best possible outcome if we executed the method beyond the termination test. Since $\epsilon_g = 10^{-1}$, we expect these values to be around 10^{-1} as well.

Considering $\|\nabla\tilde{\varphi}_{\text{ter}}^\mu\|_{(\hat{G}_{\text{ter}}^\mu)^{-1}}$ and $\|\nabla\tilde{\varphi}^\mu\|_{(\hat{G}^\mu)^{-1}}^{\text{av}}$, which report the scaled optimality measures used in the termination tests, we see that in most instances the termination test was triggered when the optimality measure $\|\nabla\tilde{\varphi}_k^\mu\|_{(\hat{G}_k^\mu)^{-1}}$ was within a factor of at most 10 of the best possible outcome. The last two columns give the two quantities in the termination test in Theorem 3.9. We can see that in all but one instance the strategy described in Remark 3.10 was able to balance the two terms, thereby tightening the tolerances and delaying a potentially too early termination. Since the derivation of the termination test relies on some conservative inequalities, we cannot expect that it can predict the smallest achievable $\|\nabla\tilde{\varphi}^\mu\|_{(\hat{G}^\mu)^{-1}}^{\text{av}}$ accurately, so in a practical setting, one may want to run the algorithm a few additional iterations after the test has been triggered. An experiment with smaller noise levels, reported in Table 4 in Appendix C, shows similar observations.

Overall, this experiment indicates that the termination test seems to be able to find a compromise between wasting unproductive iterations and taking sufficiently many iterations to reduce the optimality measure close to the best possible value.

5.2 Identification of active set

We explore whether the algorithm can identify the active constraints, as postulated in Remark 4.16. The analysis in Section 4 was done for the primal barrier method. The experiments reported here used the same primal-dual interior-point method as in the previous section. We will see that the active-set identification is also possible with that variant.

We start with a small instance of `harkerp2`,

$$\min - \sum_{i=1}^n \left(\frac{1}{2}x_i^2 + x_i \right) + \left(\sum_{i=1}^n x_i \right)^2 + 2 \sum_{j=2}^n \left(\sum_{i=j}^n x_i \right)^2 \quad \text{s.t. } x_i \geq 0, \quad \forall i \in [n], \quad (5.1)$$

with $n = 4$. The primal-dual optimal solution of this problem is $x_*^0 = (1, 0, 0, 0)^T$ and $z_*^0 = (0, 1, 1, 1)^T$, i.e., all but the first bound constraints are active at the solution and strict complementarity holds.

Figure 4 plots $\log_{10} |x_{k,i} - x_{*,i}^0|$ as a function of k when the algorithm is started from $x_0 = (1, 2, 3, 4)^T$ with $\epsilon_f = 10^{-2}$ and $\epsilon_g = \epsilon_H = 10^{-1}$. The barrier parameter is decreased by a factor of 10 every 30 iterations. Observe that, as μ decreases, $x_{k,2}, x_{k,3}, x_{k,4}$ approach their optimal value zero without much erratic behavior, whereas $x_{k,1}$, for which its optimal value is not at the boundary, keeps moving around $x_{*,1} = 1$ significantly, no matter how small μ is. This experiment provides evidence that the theoretical predictions of Remark 4.16 are observed in practice.

The final experiment examines this phenomenon for all bound-constrained examples with strictly complementary solutions. For each instance, we identified the set of active constraints for which

Table 1: Performance of the stopping test with $\mu = 10^{-1}$, $\epsilon_f = 10^{-2}$, $\epsilon_g = \epsilon_H = 10^{-1}$. **det**: number of iterations needed for noiseless instance with tolerance 10^{-6} ; **#f**: total number of function evaluations until iteration $k = \mathbf{ter}$; $\|\nabla\tilde{\varphi}_{\mathbf{ter}}^\mu\|_{\hat{G}^{-1}} = \|\nabla\tilde{\varphi}_{\mathbf{ter}}^\mu\|_{(\hat{G}_{\mathbf{ter}}^\mu)^{-1}}$; $\|\nabla\tilde{\varphi}^\mu\|^{\text{av}}$: geometric mean of $\|\nabla\tilde{\varphi}_k^\mu\|$ over the last 10 iterations, (i.e., $k = 991, \dots, 1000$) of the run; $\|\nabla\tilde{\varphi}\|_{\hat{G}^{-1}}^{\text{av}}$ is defined analogously for $\|\nabla\tilde{\varphi}_{\mathbf{ter}}^\mu\|_{\hat{G}^{-1}}$.

Problem	n	det	ter	#f	$\ \nabla\tilde{\varphi}_0^\mu\ $	$\ \nabla\tilde{\varphi}_{\mathbf{ter}}^\mu\ $	$\ \nabla\tilde{\varphi}^\mu\ ^{\text{av}}$	$\ \nabla\tilde{\varphi}_{\mathbf{ter}}^\mu\ _{\hat{G}^{-1}}$	$\ \nabla\tilde{\varphi}^\mu\ _{\hat{G}^{-1}}^{\text{av}}$	$T_{1,\mathbf{ter}}$	$T_{2,\mathbf{ter}}$
biggsb1	1000	7	5	6	3.14e+01	1.50e-01	1.42e-01	8.83e-02	8.22e-02	4.05e-01	4.05e-01
chenhark	1000	16	19	20	1.57e+01	6.40e-01	1.59e-01	1.68e+00	2.42e-01	1.81e+00	1.81e+00
cvxbqp1	100	8	6	7	2.57e+03	2.43e+00	1.45e-01	2.12e-02	3.14e-03	3.04e-01	3.04e-01
eg1	3	7	5	7	2.26e+00	5.55e-01	1.16e-01	2.32e-01	4.68e-02	3.19e-01	3.77e-01
eigena	110	21	12	14	7.28e+01	7.31e+00	2.64e-01	7.47e-01	9.83e-02	1.12e+00	1.12e+00
explin	120	18	16	17	7.65e+03	4.05e-01	1.40e-01	2.76e-02	4.57e-03	3.08e-01	3.08e-01
explin2	120	18	18	19	7.65e+03	1.44e-01	1.40e-01	3.80e-03	3.13e-03	3.02e-01	3.02e-01
expquad	120	17	16	17	7.64e+03	3.50e+00	1.40e-01	3.05e-01	4.72e-02	3.23e-01	3.23e-01
harkerp2	100	10	23	24	9.36e+06	4.32e+01	1.45e-01	2.57e-01	1.14e-02	3.77e-01	3.77e-01
mccormck	1000	14	7	8	9.38e+01	2.88e-01	1.42e-01	1.24e-01	5.87e-02	3.54e-01	3.54e-01
mdhole	2	33	15	23	2.75e+03	8.59e-01	9.53e-02	5.42e-01	2.13e-02	6.43e-01	6.43e-01
ncvxbqp1	1000	52	55	57	8.15e+01	3.35e+00	1.43e-01	2.49e-01	4.91e-02	2.13e+00	2.13e+00
ncvxbqp2	1000	108	103	104	6.01e+01	3.34e-01	1.48e-01	3.26e-01	7.68e-02	1.09e+00	1.09e+00
ncvxbqp3	1000	151	146	148	4.83e+01	1.31e+01	1.40e-01	8.83e-01	6.84e-02	2.49e+00	2.49e+00
nonscomp	1000	25	7	8	7.59e+03	5.65e-01	1.85e-01	8.77e-02	3.07e-02	7.49e-01	7.49e-01
obstclal	64	7	4	5	7.53e+00	1.99e-01	1.40e-01	1.58e-01	8.76e-02	4.67e-01	4.67e-01
obstclbl	64	6	4	5	1.95e+02	5.14e-01	1.44e-01	5.90e-02	3.60e-02	3.55e-01	3.55e-01
obstclbu	64	6	4	5	1.91e+02	3.79e-01	1.44e-01	7.10e-02	3.60e-02	3.55e-01	3.55e-01
pentdi	1000	6	3	4	1.72e+01	1.14e+00	1.42e-01	1.58e-01	3.06e-02	3.16e-01	3.16e-01
qrtquad	120	21	20	23	7.54e+03	1.35e+00	1.39e-01	7.40e-02	4.70e-02	3.23e-01	3.23e-01
qudlin	12	26	14	15	2.58e+02	3.31e+00	2.11e-01	2.64e-01	1.15e-01	7.40e-01	7.40e-01
sim2bqp	2	7	4	5	4.02e+01	3.37e-01	6.08e-02	8.65e-02	2.00e-02	3.40e-01	3.40e-01

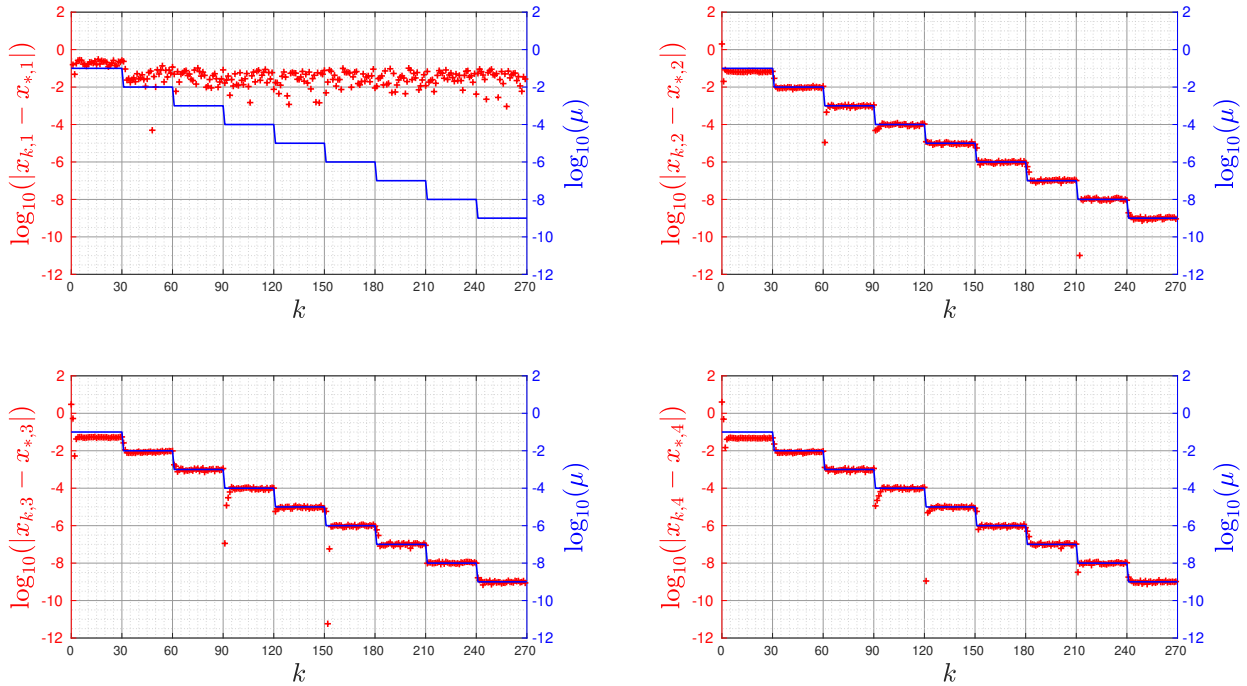


Figure 4: `harkerp2`. $\log_{10} |x_i - x_{*,i}^0|$ for $i \in [4]$.

strict complementarity holds, i.e., $\mathcal{A}_s = \{i \in \mathcal{A} : z_{*,i}^0 > 0\}$ (for details see Table 3 in Appendix A). The data for Table 2 was generated from the last 10 iterates after running the algorithm for 5000 iterations, which is long enough to reach asymptotic behavior even for very small values of μ . As we proved in Section 4, $\|x_{k,\mathcal{A}_s}^\mu\|$ converges to zero as $\mu \rightarrow 0$, and it does so at the same rate as μ , which is expected due to $z_{*,i}^\mu; x_{*,i}^\mu = \mu$.

5.3 Update of the barrier parameter

In order to solve the original problem (1.1), we are interested in obtaining a good solution of the barrier problem (in the sense of Theorem 3.9) for a target value $\bar{\mu} > 0$ that is small enough so that the barrier term does not push the iterates too far from the boundary of the feasible region. If one is interested in identifying which variables are at their bound, a very small value of $\bar{\mu}$ should be chosen, as discussed in the previous section. On the other hand, if the active constraints are not of interest, it is not clear that decreasing μ_ℓ below a moderate value related to the noise level is advantageous since the non-active variables remain affected by the noise and dominate the effect on the objective function.

In practice, starting the optimization with the final target value, e.g., $\bar{\mu} = 10^{-7}$, may lead to an extremely large number of iterations before convergence, a phenomenon that we also observed in our experiments in the noisy setting. In the non-noisy setting, a practical interior-point method starts with a large initial value of μ_0 and solves a sequence of barrier problems approximately, for decreasing values of μ_ℓ . The approximate solution of the barrier problem for μ_ℓ then provides a good starting point for solving the next barrier problem with $\mu_{\ell+1}$.

In the non-noisy setting, μ_ℓ is decreased whenever an optimality measure is below a fraction of μ_ℓ . However, this approach cannot be applied here because the best-achievable tolerance, the

Table 2: Behavior of the non-degenerate active variable iterates x_{k, \mathcal{A}_s}^μ over the last 10 iterations. (* Converged to a different local solution.)

Problem	max. of $\ x_{k, \mathcal{A}_s}^\mu\ _\infty$ in last 10 iterations.			
	$\epsilon_f = 10^{-2}, \epsilon_g = \epsilon_H = 10^{-1}$		$\epsilon_f = 10^{-6}, \epsilon_g = \epsilon_H = 10^{-3}$	
	$\mu = 10^{-4}$	$\mu = 10^{-8}$	$\mu = 10^{-4}$	$\mu = 10^{-8}$
chenhark	1.05e-04	1.01e-08	1.05e-04	1.00e-08
cvxbqp1	8.45e-05	8.45e-09	8.33e-05	8.33e-09
eg1	2.76e-04	1.46e-08	1.99e-04	1.28e-08
explin	1.30e-05	1.30e-09	1.30e-05	1.30e-09
explin2	1.03e-05	1.03e-09	1.03e-05	1.03e-09
expquad	1.00e-05	1.00e-09	1.00e-05	1.00e-09
harkerp2	1.03e-04	1.07e-08	9.88e-05	1.00e-08
mccormck	1.07e-04	1.07e-08	1.07e-04	1.07e-08
mdhole	1.16e-04	1.16e-08	1.00e-04	1.00e-08
ncvxbqp1	2.22e-03	2.20e-07	1.97e-03	1.97e-07
ncvxbqp2	2.10e-03	2.10e-07	1.97e-03	1.97e-07
ncvxbqp3	5.44e-02	3.31e-06	2.42e-02	2.82e-06
obstclal	5.76e-03	7.58e-07	3.13e-03	3.55e-07
obstclbl	3.29e-03	1.09e-06	2.63e-03	4.37e-07
obstclbu	3.29e-03	1.09e-06	2.63e-03	4.37e-07
pentdi	4.36e-04	4.00e-08	4.26e-04	4.00e-08
qrtquad	1.01e-05	1.01e-09	1.01e-05	1.36e-01*
qudlin	6.63e-06	1.00e-09	1.00e-05	1.00e-09
sim2bqp	1.11e-04	1.11e-08	1.00e-04	1.00e-08

right-hand-side of (3.8), does not decrease to zero as $\mu_\ell \rightarrow 0$.

In experiments that are reported in Appendix E, we explored a heuristic that decreases the barrier parameter whenever the stopping test in Remark 3.10 holds and $\|X_k^{\mu_\ell} z_k^{\mu_\ell} - \mu_\ell e\|_\infty \leq \kappa_\mu \mu_\ell$ for some $\kappa_\mu \in (0, 1)$, or a fixed number N_μ of iterations for μ_ℓ are exceeded. With this procedure, solutions of (2.1) with $\bar{\mu} = 10^{-7}$ could be computed in a reasonable number of iterations.

6 Concluding remarks

The goal of this paper is to provide a first step towards understanding the impact of the barrier term on the convergence properties of an interior-point algorithm for problem instances with bounded noise. By relaxing only the Armijo line-search condition, we keep the method very similar to the standard interior-point framework used in the non-noisy setting so that existing implementations can be easily adjusted. To keep the initial analysis manageable, we restricted our focus to problems that have only bound constraints. As a next step, we will explore interior-point methods for noisy instances with general inequality constraints. We conjecture that active-set identification can also be observed in this context.

We point out that the practical termination test introduced in Section 3.2 is not limited to the interior-point setting. The methodology of estimating the unknown problem-dependent parameters in a theoretical convergence theorem like Theorem 3.8 by quantities observed during the run of the algorithm can also be applied to methods with similar formulations of a global convergence result, such as in [18, 23].

Acknowledgement

We thank Jorge Nocedal and Frank E. Curtis for inspiring conversations that helped us to improve the work presented here.

References

- [1] A. S. BERAHAS, R. H. BYRD, AND J. NOCEDAL, *Derivative-free optimization of noisy functions via quasi-Newton methods*, SIAM Journal on Optimization, 29 (2019), pp. 965–993.
- [2] A. S. BERAHAS, L. CAO, AND K. SCHEINBERG, *Global convergence rate analysis of a generic line search algorithm with noise*, SIAM Journal on Optimization, 31 (2021), pp. 1489–1518.
- [3] A. S. BERAHAS, F. E. CURTIS, D. ROBINSON, AND B. ZHOU, *Sequential quadratic optimization for nonlinear equality constrained stochastic optimization*, SIAM Journal on Optimization, 31 (2021), pp. 1352–1379.
- [4] J. BLANCHET, C. CARTIS, M. MENICKELLY, AND K. SCHEINBERG, *Convergence rate analysis of a stochastic trust-region method via supermartingales*, INFORMS Journal on Optimization, 1 (2019), pp. 92–119.
- [5] I. BONGARTZ, A. R. CONN, N. GOULD, AND P. L. TOINT, *CUTE: Constrained and unconstrained testing environment*, ACM Transactions on Mathematical Software (TOMS), 21 (1995), pp. 123–160.
- [6] R. H. BYRD, J. C. GILBERT, AND J. NOCEDAL, *A trust region method based on interior point techniques for nonlinear programming*, Mathematical Programming, 89 (2000), pp. 149–185.
- [7] R. H. BYRD, M. E. HRIBAR, AND J. NOCEDAL, *An interior point algorithm for large-scale nonlinear programming*, SIAM Journal on Optimization, 9 (1999), pp. 877–900.
- [8] L. CAO, A. S. BERAHAS, AND K. SCHEINBERG, *First- and second-order high probability complexity bounds for trust-region methods with noisy oracles*, Mathematical Programming, (2023), pp. 1–52.
- [9] F. E. CURTIS, V. KUNGURTSEV, D. P. ROBINSON, AND Q. WANG, *A stochastic-gradient-based interior-point algorithm for solving smooth bound-constrained optimization problems*, arXiv preprint arXiv:2304.14907, (2023).
- [10] F. E. CURTIS, D. P. ROBINSON, AND B. ZHOU, *Inexact sequential quadratic optimization for minimizing a stochastic objective function subject to deterministic nonlinear equality constraints*, arXiv preprint arXiv:2107.03512, (2021).
- [11] F. E. CURTIS, D. P. ROBINSON, AND B. ZHOU, *Sequential quadratic optimization for stochastic optimization with deterministic nonlinear inequality and equality constraints*, arXiv preprint arXiv:2302.14790, (2023).
- [12] F. E. CURTIS, K. SCHEINBERG, AND R. SHI, *A stochastic trust region algorithm based on careful step normalization*, INFORMS Journal on Optimization, 1 (2019), pp. 200–220.
- [13] C. KELLEY, *Newton’s method in mixed precision*, SIAM Review, 64 (2022), pp. 191–211.

- [14] J. J. MOREÉ AND S. M. WILD, *Estimating computational noise*, SIAM Journal on Scientific Computing, 33 (2011), pp. 1292–1314.
- [15] S. NA, M. ANITESCU, AND M. KOLAR, *Inequality constrained stochastic nonlinear optimization via active-set sequential quadratic programming*, Mathematical Programming, (2023), pp. 1–75.
- [16] L. W. NG AND K. E. WILLCOX, *Multifidelity approaches for optimization under uncertainty*, International Journal for Numerical Methods in Engineering, 100 (2014), pp. 746–772.
- [17] J. NOCEDAL AND S. J. WRIGHT, *Numerical optimization*, Springer, 1999.
- [18] F. OZTOPRAK, R. BYRD, AND J. NOCEDAL, *Constrained optimization in the presence of noise*, SIAM Journal on Optimization, 33 (2023), pp. 2118–2136.
- [19] C. PAQUETTE AND K. SCHEINBERG, *A stochastic line search method with expected complexity analysis*, SIAM Journal on Optimization, 30 (2020), pp. 349–376.
- [20] S. QIU AND V. KUNGURTSEV, *A sequential quadratic programming method for optimization with stochastic objective functions, deterministic inequality constraints and robust subproblems*, arXiv preprint arXiv:2302.07947, (2023).
- [21] K. SCHEINBERG AND M. XIE, *Stochastic adaptive regularization method with cubics: A high probability complexity bound*, in OPT 2022: Optimization for Machine Learning (NeurIPS 2022 Workshop), 2022.
- [22] H.-J. M. SHI, Y. XIE, R. BYRD, AND J. NOCEDAL, *A noise-tolerant quasi-Newton algorithm for unconstrained optimization*, SIAM Journal on Optimization, 32 (2022), pp. 29–55.
- [23] S. SUN AND J. NOCEDAL, *A trust region method for noisy unconstrained optimization*, Mathematical Programming, (2023), pp. 1–28.
- [24] R. J. VANDERBEI, *Nonlinear optimization models.*, <https://vanderbei.princeton.edu/ampl/nlmodels/>.
- [25] A. WÄCHTER AND L. T. BIEGLER, *Line search filter methods for nonlinear programming: Motivation and global convergence*, SIAM Journal on Optimization, 16 (2005), pp. 1–31.
- [26] A. WÄCHTER AND L. T. BIEGLER, *On the implementation of an interior-point filter line-search algorithm for large-scale nonlinear programming*, Mathematical Programming, 106 (2006), pp. 25–57.
- [27] S. J. WRIGHT AND D. ORBAN, *Properties of the log-barrier function on degenerate nonlinear programs*, Mathematics of Operations Research, 27 (2002), pp. 585–613.
- [28] Y. XIE, R. H. BYRD, AND J. NOCEDAL, *Analysis of the BFGS method with errors*, SIAM Journal on Optimization, 30 (2020), pp. 182–209.
- [29] H. YAMASHITA, *A globally convergent primal-dual interior point method for constrained optimization*, Optimization Methods and Software, 10 (1998), pp. 443–469.
- [30] H. YAMASHITA, H. YABE, AND T. TANABE, *A globally and superlinearly convergent primal-dual interior point trust region method for large scale constrained optimization*, Mathematical Programming, 102 (2005), pp. 111–151.

A Indices of non-degenerate and degenerate active constraints, inactive constraints, and free variables

In Table 3, we provide the number of non-degenerate and degenerate active constraints, inactive constraints, and free variables, along with their corresponding indices, for the test problems discussed in Section 5. This is particularly relevant for replicating the results in Table 2. In order to determine which bound constraints are active, we run IPOPT to solve the non-noisy problems and examine the value of the primal and dual variables. If the dual variables are nonzero for the variables that their optimal value is at the boundary of the feasible region, we consider those bound constraints active.

Table 3: Indices and number of non-degenerate, degenerate, inactive, and free variables

Problem	n	non-deg. act. vars		deg. act. vars		bnd. & inact. vars		free vars	
		ct	\mathcal{A}_s	ct	\mathcal{A}_d	ct	\mathcal{I}_b	ct	\mathcal{I}_f
biggsb1	1000	0	\emptyset	999	[999]	0	\emptyset	1	{1000}
chenhark	1000	300	{701, ..., 1000}	200	{501, ..., 700}	500	[500]	0	\emptyset
cvxbqp1	100	100	{1, ..., 100}	0	\emptyset	0	\emptyset	0	\emptyset
eg1	3	1	{3}	0	\emptyset	1	{2}	1	{1}
eigena	110	0	\emptyset	90	[110] \ \mathcal{I}_b	20	{1, 2, 12, 14, 23, 26, 34, 38, 45, 50, 56, 62, 67, 74, 78, 86, 89, 98, 100, 110}	0	\emptyset
explin	120	115	[120] \ \mathcal{I}_b	0	\emptyset	5	{2, 4, 6, 8, 10}	0	\emptyset
explin2	120	117	[120] \ \mathcal{I}_b	0	\emptyset	3	{6, 8, 10}	0	\emptyset
expquad	120	10	[10]	0	\emptyset	0	\emptyset	110	[120] \ \mathcal{A}_s
harkerp2	100	99	{2, ..., 100}	0	\emptyset	1	{1}	0	\emptyset
mccormck	1000	1	{1000}	0	\emptyset	999	[999]	0	\emptyset
mdhole	2	1	{1}	0	\emptyset	0	\emptyset	1	{2}
ncvxbqp1	1000	1000	[1000]	0	\emptyset	0	\emptyset	0	\emptyset
ncvxbqp2	1000	992	[1000] \ \mathcal{I}_b	0	\emptyset	8	{146, 248, 266, 302, 338, 428, 446, 464}	0	\emptyset
ncvxbqp3	1000	987	[1000] \ \mathcal{I}_b	0	\emptyset	13	{3, 352, 388, 406, 424, 442, 460, 478, 496, 536, 548, 722, 740, 746}	0	\emptyset
nonscomp	1000	0	\emptyset	316	{3, 6, 9, ..., 948}	684	[1000] \ \mathcal{A}_d	0	\emptyset
obstclal	64	27	{11, ..., 14, 18, ..., 23, 26 ... 31, 34, ..., 39, 42, ..., 46}	0	\emptyset	37	[64] \ \mathcal{A}_s	0	\emptyset
obstclbl	64	48	[64] \ \mathcal{I}_b	0	\emptyset	16	{4, 5, 12, 13, 25, 26, 31, 32, 33, 34, 39, 40, 52, 53, 60, 61}	0	\emptyset
obstclbu	64	48	[64] \ \mathcal{I}_b	0	\emptyset	16	{4, 5, 12, 13, 25, 26, 31, 32, 33, 34, 39, 40, 52, 53, 60, 61}	0	\emptyset
pentdi	1000	502	{3, 498, 501, 502, ..., 1000}	496	[1000] \ ($\mathcal{A}_s \cup \mathcal{I}_b$)	2	{1, 500}	0	\emptyset
qrtquad	120	5	{1, 3, 5, 7, 9}	0	\emptyset	115	[120] \ \mathcal{A}_s	0	\emptyset
qudlin	12	10	{3, ..., 12}	0	\emptyset	2	{1, 2}	0	\emptyset
sim2bqp	2	1	{2}	0	\emptyset	0	\emptyset	1	{1}

B Uniform Lower Bound on the step size in Lemma 4.12

Lemma B.1. Consider $\phi(\alpha) = a\alpha^2 + b\alpha - c$ in Lemma 4.12. The positive root of $\phi(\alpha)$, i.e., $\alpha_k = \frac{-b + \sqrt{b^2 + 4ac}}{2a}$ is a decreasing function of a and b .

Proof. The partial derivative of α_k with respect to a is given by

$$\frac{\partial \alpha_k}{\partial a} = \frac{b - \frac{2ac + b^2}{\sqrt{4ac + b^2}}}{2a^2},$$

observe that $b - \frac{2ac + b^2}{\sqrt{4ac + b^2}} \leq 0$ because $4a^2c^2 \geq 0$. Thus, α_k is a decreasing function of a . The partial derivative of α_k with respect to b is given by

$$\frac{\partial \alpha_k}{\partial b} = \frac{\frac{b}{\sqrt{4ac + b^2}} - 1}{2a},$$

observe that $\frac{b}{\sqrt{4ac + b^2}} - 1 \leq 0$ because $4ac \geq 0$. Thus, α_k is a decreasing function of b . \square

C Further numerical results on the barrier subproblem

In this appendix, we provide additional numerical results concerning the effectiveness of the stopping test outlined in Theorem 3.9 with a smaller noise level. We observe a similar algorithmic behavior to that provided in Table 1.

Table 4: Performance of the stopping test with $\mu = 10^{-1}$, $\epsilon_f = 10^{-6}$, $\epsilon_g = \epsilon_H = 10^{-3}$, $\nu = 10^{-6}$.

Problem	n	ter	#f	$\ \nabla \tilde{\varphi}_0^\mu\ $	$\ \nabla \tilde{\varphi}_{\text{ter}}^\mu\ $	$\ \nabla \tilde{\varphi}^\mu\ ^{\text{av}}$	$\ \nabla \tilde{\varphi}_{\text{ter}}^\mu\ _{\hat{G}^{-1}}$	$\ \nabla \tilde{\varphi}^\mu\ _{\hat{G}^{-1}}^{\text{av}}$	$T_{1,\text{ter}}$	$T_{2,\text{ter}}$
biggsb1	1000	5	6	3.14e+01	4.27e-03	1.42e-03	2.46e-03	8.20e-04	4.02e-03	4.02e-03
chenhark	1000	271	287	1.57e+01	1.90e-02	1.05e-02	8.67e-01	1.85e-01	1.26e+00	1.26e+00
cvxbqp1	100	7	8	2.57e+03	1.50e-03	1.45e-03	2.25e-05	3.13e-05	3.04e-03	3.04e-03
egl	3	6	7	2.36e+00	1.13e-03	1.15e-03	6.91e-04	4.84e-04	3.67e-03	3.67e-03
eigena	110	19	21	7.28e+01	1.21e-01	1.40e-03	8.77e-03	1.18e-03	1.07e-02	1.07e-02
explin	120	17	18	7.65e+03	1.41e-03	1.40e-03	5.82e-05	4.56e-05	3.08e-03	3.08e-03
explin2	120	17	18	7.65e+03	1.41e-03	1.40e-03	2.74e-05	3.13e-05	3.02e-03	3.02e-03
expquad	120	15	16	7.64e+03	5.30e-02	1.40e-03	1.17e-03	4.71e-04	3.23e-03	3.23e-03
harkerp2	100	10	11	9.36e+06	9.41e-03	1.45e-03	1.26e-04	1.16e-04	3.79e-03	3.79e-03
mccormck	1000	7	8	9.38e+01	1.37e-03	1.42e-03	5.68e-04	5.87e-04	3.53e-03	3.53e-03
mdhole	2	29	49	2.75e+03	7.39e-04	1.48e-03	2.78e-04	3.65e-04	3.33e-03	3.33e-03
ncvxbqp1	1000	51	52	8.15e+01	3.08e-03	1.42e-03	1.80e-04	1.75e-04	9.35e-03	9.35e-03
ncvxbqp2	1000	107	108	6.01e+01	1.42e-03	1.42e-03	6.00e-04	4.43e-04	1.11e-02	1.11e-02
ncvxbqp3	1000	146	147	4.83e+01	1.75e-02	1.39e-03	2.16e-03	6.59e-04	1.54e-02	1.54e-02
nonscomp	1000	7	14	7.59e+03	9.17e+00	1.61e-03	1.14e+00	7.66e-04	1.24e+00	1.24e+00
obstclal	64	5	6	7.54e+00	4.87e-03	1.42e-03	4.04e-03	8.43e-04	4.65e-03	4.65e-03
obstclbl	64	5	6	1.95e+02	2.09e-03	1.43e-03	8.25e-04	3.60e-04	3.55e-03	3.55e-03
obstclbu	64	5	6	1.91e+02	2.19e-03	1.43e-03	7.31e-04	3.60e-04	3.55e-03	3.55e-03
pentdi	1000	5	6	1.72e+01	1.45e-03	1.42e-03	3.15e-04	3.06e-04	3.17e-03	3.17e-03
qrtquad	120	19	22	7.54e+03	1.84e-03	1.39e-03	4.99e-04	4.70e-04	3.23e-03	3.23e-03
qudlin	12	24	30	2.58e+02	1.04e-02	1.25e-03	7.57e-03	8.64e-04	8.19e-03	8.19e-03
sim2bqp	2	5	6	4.03e+01	8.57e-03	1.30e-03	1.73e-03	5.11e-04	3.39e-03	3.39e-03

D Numerical observation: Impact of gradient noise distribution on non-noisy gradient

In this appendix, we share an observation related to the non-noisy gradient at the final iterations of the algorithm. Depending on the specific distribution of the randomly added noise to generate the noisy gradient, we see an interesting pattern in the non-noisy gradient.

We consider the following optimization problem

$$\min_{x \in \mathbb{R}^n} \frac{c_1}{2} (x_1 - 1)^2 + c_2 \cdot x_2 \quad \text{s.t.} \quad x \geq 0, \quad (\text{D.1})$$

where values of the coefficients c_1 and c_2 are specified in each example. For all the following experiments, noise in the objective function follows a Bernoulli distribution with parameter of 0.5 and magnitude of $\epsilon_f = 10^{-2}$ and the diagonal elements of the Hessian are perturbed with a Bernoulli distributed noise with parameter 0.5 and magnitude $\epsilon_H = 10^{-1}$. The distribution of the noise in the gradient is specified in each example respectively, where $\epsilon_g = 10^{-1}$. In each example, we solve the barrier subproblem with $\mu = 10^{-8}$ and run the algorithm for 1000 iterations. The scatter plots of the iterates x_2 versus x_1 , the noisy gradient $\nabla_{x_2} \tilde{\varphi}$ versus $\nabla_{x_1} \tilde{\varphi}$, and the deterministic gradient $\nabla_{x_2} \varphi$ versus $\nabla_{x_1} \varphi$ are provided for the last 200 iterations of the run of the algorithm (See Figures 5, 6, 7, and 8).

Example D.1. *Let $c_1 = c_2 = 1$ in problem (D.1). Noise in the gradient is uniformly distributed on the surface of a 2-dimensional circle with radius ϵ_g around the deterministic gradient.*

In Figure 5, we observe that the points (x_1, x_2) are scattered around an ellipse. Since $x_{2,} = 0$, the ellipse is narrower in the x_2 direction. In addition, (x_1, x_2) 's have denser concentrations around the circumference of the ellipse. We further observe that $(\nabla_{x_1} \tilde{\varphi}, \nabla_{x_2} \tilde{\varphi})$'s are scattered uniformly in a circle with radius $\approx 10^{-1}$. In addition, the deterministic gradient $(\nabla_{x_1} \varphi, \nabla_{x_2} \varphi)$'s are densely concentrated around the circumference of a circle with radius $\approx 10^{-1}$.*

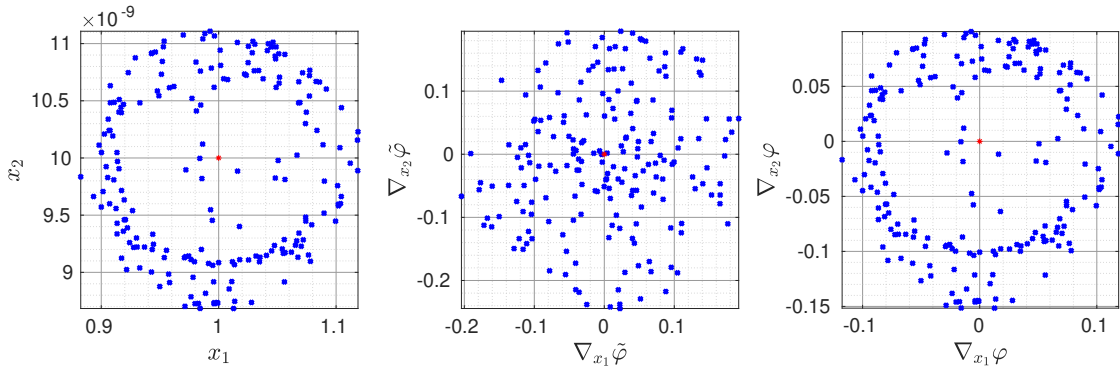


Figure 5: Example D.1 observation

Example D.2. *Let $c_1 = c_2 = 1000$ in problem (D.1). Noise in the gradient is uniformly distributed on the surface of a 2-dimensional circle with radius ϵ_g around the deterministic gradient.*

In Figure 6, we observe similar phenomena as in Example D.1 and Figure 5. The concentrations of points (x_1, x_2) and $(\nabla_{x_1} \varphi, \nabla_{x_2} \varphi)$ around the circumferences of the ellipse and circle are even more pronounced. This is due to the scaling of the problem with $c_1 = c_2 = 1000$. Comparing the range of

the axes of the scatter plots of x_2 versus x_1 in Figures 5 and 6 suggests that this scaling results in a more accurate solution.

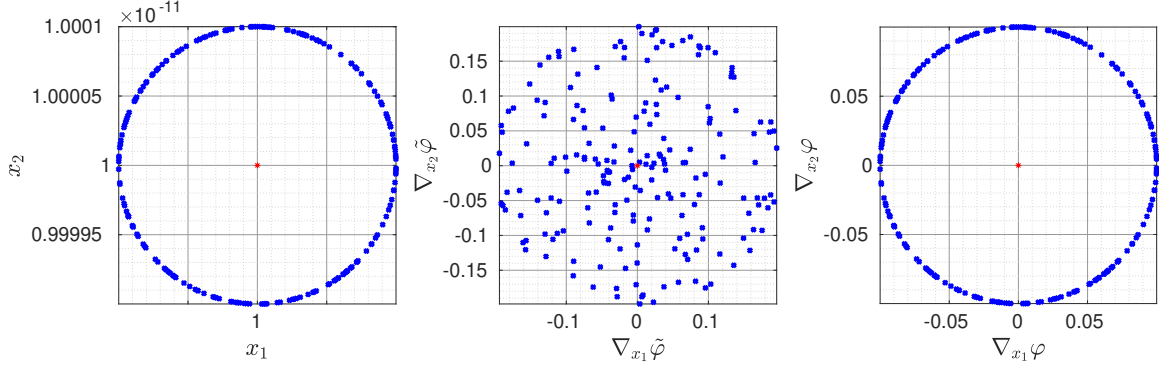


Figure 6: Example D.2 observation

Example D.3. Let $c_1 = c_2 = 1$ in problem (D.1). Each element of the gradient is perturbed with a uniformly distributed noise with support $[-\epsilon_g, \epsilon_g]$.

In Figure 7, we observe that the points (x_1, x_2) are scattered in a rectangle and since $x_{2,*} = 0$, the rectangle is narrower in the x_2 direction. We further observe that $(\nabla_{x_1} \tilde{\varphi}, \nabla_{x_2} \tilde{\varphi})$ and $(\nabla_{x_1} \varphi, \nabla_{x_2} \varphi)$'s are scattered uniformly in a square/rectangle where the length of the edges is close to 0.1.

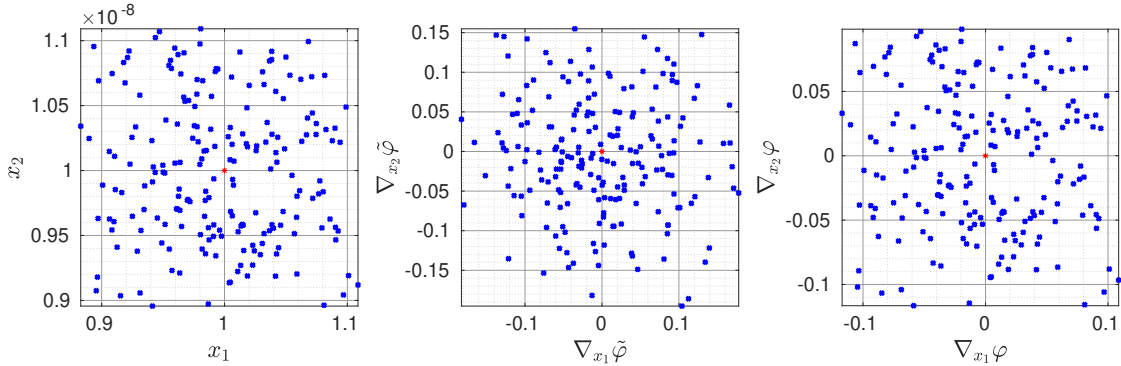


Figure 7: Example D.3 observation

Example D.4. Let $c_1 = c_2 = 1000$ in problem (D.1). Each element of the gradient is perturbed with a uniformly distributed noise with support $[-\epsilon_g, \epsilon_g]$.

In Figure 8, we have a similar observation as in Example D.3 and Figure 7. Again, comparing the range of the axes in the scatter plots of x_2 versus x_1 in Figures 7 and 8 suggests that this scaling results in a more accurate solution.

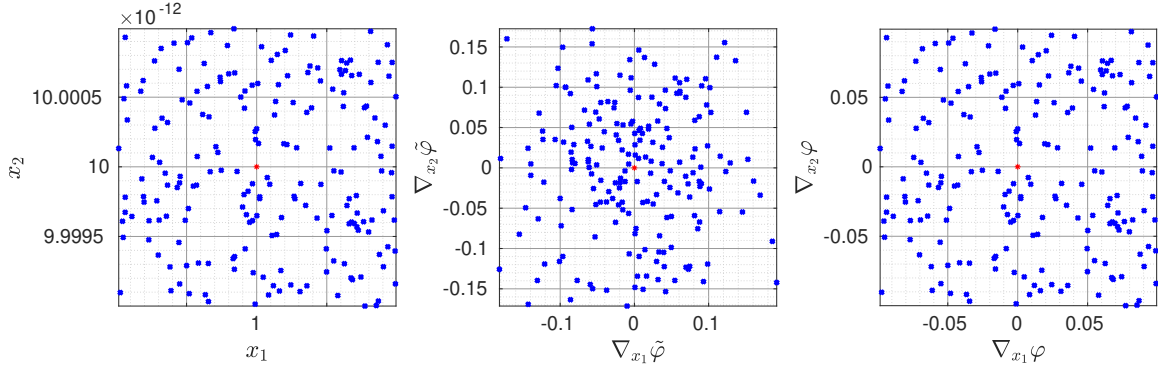


Figure 8: Example D.4 observation

E Numerical results on the barrier parameter update rule

In this appendix, we propose a heuristic for updating the barrier parameter μ in order to solve problem (1.1) in the interior-point method framework and illustrate its effectiveness by providing numerical experiments.

As mentioned in Section 5, we observed that the primal-dual implementation improves the convergence behavior of the algorithm significantly compared to the primal approach. Thus, the implemented algorithm follows the primal-dual approach, as presented in Algorithm 2. This algorithm consists of two loops: the outer *for loop* and the inner *while loop*. The overall algorithm stops when the barrier parameter becomes smaller than a μ_{\min} . Ignoring the stopping condition of the inner while loop, this loop can be viewed as the primal-dual implementation of Algorithm 1 for a fixed $\mu = \mu_\ell$. Hence, all experiments conducted with a fixed μ , as presented in Section 5, correspond to the inner while loop of Algorithm 2.

Before presenting the results of the numerical experiments, let us briefly review Algorithm 2. At the beginning of each iteration j of the outer for loop, the fraction-to-the-boundary rule parameter τ_ℓ is updated [26] in line 2. Then, the while loop condition checks whether the barrier subproblem is solved to a prescribed desired accuracy. If the condition is met, then the barrier parameter is updated in line 12. In addition, the iterates and iteration counter (for the inner loop) are reset in lines 13 and 14, respectively. Conversely, if the condition is not met, in iteration k of the inner while loop, the steps d_k and d_k^z are defined as the solutions of the linear system

$$\begin{bmatrix} \tilde{H}_k^\mu & -I \\ Z_k^\mu & X_k^\mu \end{bmatrix} \begin{bmatrix} d_k \\ d_k^z \end{bmatrix} = - \begin{bmatrix} \tilde{g}_k^\mu - z_k^\mu \\ X_k^\mu z_k^\mu - \mu e \end{bmatrix}. \quad (\text{E.1})$$

To compute d_k and d_k^z , we multiply the second row of (E.1) by $(X_k^\mu)^{-1}$ and add up both rows to obtain

$$\left(\tilde{H}_k^\mu + (X_k^\mu)^{-1} Z_k^\mu \right) d_k = -(\tilde{g}_k^\mu - \mu (X_k^\mu)^{-1} e). \quad (\text{E.2})$$

As we already discussed in Section 5, we ensure that the $\tilde{H}_k^\mu + (X_k^\mu)^{-1} Z_k^\mu$ is positive definite by adding a multiple of the identity matrix to it before calculating the step d_k . After finding d_k by solving (E.2), we proceed to compute d_k^z by

$$d_k^z = -(X_k^\mu)^{-1} (Z_k^\mu d_k - \mu e) - z_k^\mu. \quad (\text{E.3})$$

Algorithm 2 : Interior-point with relaxed line search for solving problem (1.1)

Require: $\nu \in (0, \frac{1}{2})$; $\epsilon_R > 2\epsilon_f$; $\tau_{\min} \in (0, 1)$; $N_\mu = 10$; $\kappa_\mu = 10$; $\kappa_{\text{dec}} = 0.1$; $\kappa_\Sigma = 10^4$; $\mu_{\min} \in (0, 1)$;
 Initial iterate $x_0 \in \mathbb{R}^n$; Initial dual variables $z_0 \in \mathbb{R}^{n_u}$, $\mu_0 \in \mathbb{R}_{>0}$.

- 1: **for** $\ell = 0, 1, \dots$ **do**
- 2: Set $\tau_\ell \leftarrow \max\{\tau_{\min}, 1 - \mu_\ell\}$.
- 3: **while** a prescribed stopping condition is not satisfied **do**
- 4: Compute d_k and d_k^z by (E.2) and (E.3), respectively.
- 5: Compute α_k^{\max} by (2.7) and α_k^{dual} by (E.4) with $\mu = \mu_\ell$ and $\tau = \tau_\ell$.
- 6: Set $\alpha_k \leftarrow \left(\frac{1}{2}\right)^i \alpha_k^{\max}$ (i : smallest element of \mathbb{N} yielding (2.8) with $\mu = \mu_\ell$).
- 7: Set $x_{k+1}^{\mu_\ell} \leftarrow x_k^{\mu_\ell} + \alpha_k d_k$, and $z_{k+1}^{\mu_\ell} \leftarrow z_k^{\mu_\ell} + \alpha_k^{\text{dual}} d_k^z$.
- 8: Reset $z_{k+1}^{\mu_\ell}$ according to (E.5).
- 9: Set $k \leftarrow k + 1$.
- 10: **end while**
- 11: **if** $\mu_\ell \leq \mu_{\min}$ **then** Stop. **end if**
- 12: Set $\mu_{\ell+1} \leftarrow \kappa_{\text{dec}} \mu_\ell$.
- 13: Set $x_0^{\mu_{\ell+1}} \leftarrow x_k^{\mu_\ell}$, and $z_0^{\mu_{\ell+1}} \leftarrow z_k^{\mu_\ell}$.
- 14: Set $k \leftarrow 0$.
- 15: **end for**

Next, the fraction-to-the-boundary rule determines the upper bound on the step sizes in d_k and d_k^z directions. The upper bound on the primal step size, α_k^{\max} , is defined similar to (2.7) with $\tau = \tau_\ell$. As for the upper bound on the dual step size, we define α_k^{dual} as follows

$$\alpha_k^{\text{dual}} := \max \left\{ \alpha \in (0, 1] : z_k^\mu + \alpha d_k^z \geq (1 - \tau_\ell) z_k^\mu \right\} \quad (\text{E.4})$$

with $\tau_\ell \in (0, 1)$. Subsequently, α_k is determined in line 6 and the primal and dual iterates are updated in line 7. Following [26], to prevent the primal-dual Hessian $\tilde{H}_k^\mu + (X_k^\mu)^{-1} Z_k^\mu$ from deviating significantly from the primal Hessian $\tilde{G}_k^\mu = \tilde{H}_k^\mu + \mu (X_k^\mu)^{-2}$, the dual variables are projected as

$$z_{k+1,i}^\mu \leftarrow \max \left\{ \min \left\{ z_{k+1,i}^\mu, \frac{\kappa_\Sigma \mu_\ell}{x_{k+1,i}^\mu} \right\}, \frac{\mu_\ell}{\kappa_\Sigma x_{k+1,i}^\mu} \right\}, \quad \text{for } i \in [n], \quad (\text{E.5})$$

where $\kappa_\Sigma \geq 1$.

In the remainder of this appendix, we present numerical results regarding the performance of the overall Algorithm 2 for solving problem (1.1) and the importance of the heuristic for decreasing the barrier parameter.

As discussed in Section 3.10, for good practical performance it is important to start the algorithm with a relatively large value of μ_0 (such as 0.1) and only decrease the barrier parameter when the corresponding barrier problem has been solved sufficiently accurately. The stopping test in Theorem 3.9 provides an upper bound on the smallest values of the scaled norm of the gradient of the barrier function upon that can be achieved. This condition naturally suggests to reduce the barrier parameter as soon as condition (i) or (ii) is satisfied, i.e., whenever $\|\nabla \tilde{\varphi}^\mu(x_k^\mu)\|_{(\tilde{G}_k^\mu)^{-1}} \leq \max\{T_{1,k}, T_{2,k}\}$ with $T_{1,k}$ and $T_{2,k}$ defined in (3.13). However, the upper bound $\max\{T_{1,k}, T_{2,k}\}$ is based on pessimistic assumptions on the error in the function. More importantly, the tolerances do not become tighter as μ decreases and the termination test might get triggered very quickly after an update of μ_ℓ even though not enough iterations have been taken to solve the new barrier problem well. We demonstrate this issue in Figure 9. We use j to indicate the accumulation of the total

number of iterations that Algorithm 2 has executed, i.e., the total number of outer and inner loops iterations.

Figure 9 presents the plot of $\log_{10}(\|x_{j,\mathcal{A}_s} - x_{*,\mathcal{A}_s}\|_\infty)$ against the iteration number j on the left vertical axis, and the plot of $\log_{10}(\mu)$ against j on the right vertical axis. Using the stopping test described in Theorem 3.9 the barrier parameter is decreased for the first time in iteration 23. Subsequently, it is decreased in every iteration until reaching its minimum value in iteration 30. Thus, if the termination test in Theorem 3.9 is utilized, the algorithm stops in iteration 31, shown by the dashed vertical line, where $\|x_{j,\mathcal{A}_s} - x_{*,\mathcal{A}_s}\|_\infty$ is approximately 10^{-6} . However, if we continue running the algorithm, $\|x_{j,\mathcal{A}_s} - x_{*,\mathcal{A}_s}\|_\infty$ decreases to 10^{-8} , yielding a more accurate solution. Thus, the stopping condition in Theorem 3.9 is satisfied in every iteration after being satisfied once, leading to early termination of the algorithm.

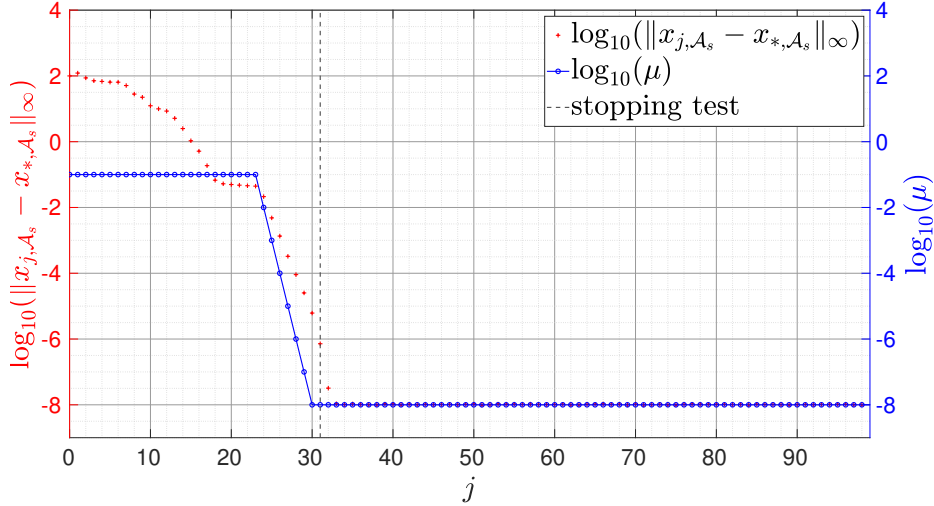


Figure 9: $\log_{10}(\|x_{j,\mathcal{A}_s} - x_{*,\mathcal{A}_s}\|_\infty)$ and $\epsilon_f = 10^{-2}$, $\epsilon_g = \epsilon_H = 10^{-1}$ for **harkerp2** (stopping test)

To address this issue, we turn to the deterministic setting where the norm of the KKT residuals is used as the criterion for updating the barrier parameter, i.e., μ is decreased if

$$\max \{ \|\nabla f_k^\mu - z_k^\mu\|_\infty, \|X_k^\mu z_k^\mu - \mu e\|_\infty \} \leq \kappa_\mu \mu,$$

for a prescribed constant $\kappa_\mu \in \mathbb{R}_{>0}$ [26]. Following the deterministic approach and by adopting the primal-dual point of view of interior-point methods, we propose a heuristic that combines the stopping test described in Theorem (3.9) with the norm of the perturbed complementarity condition, i.e., $\|Xz - \mu e\|_\infty$. We define the following two conditions, i.e., C1 and C2

$$\text{C1. } \|\nabla \tilde{\varphi}_k^\mu\|_{(\hat{G}_k^\mu)^{-1}} \leq \max \{T_{1,k}, T_{2,k}\} + \kappa_\mu \mu,$$

$$\text{C2. } \|X_k^\mu z_k^\mu - \mu e\|_\infty \leq \kappa_\mu \mu,$$

and the barrier parameter is decreased if these two conditions are satisfied with $\mu = \mu_\ell$. In other words, these two conditions serve as the stopping condition for the while loop in line 3 of Algorithm 2. Observe that since $\nabla f_k^\mu - z_k^\mu \approx \nabla \varphi_k^\mu$, Condition C1 mimics $\|\nabla f(x_k^\mu) - z_k^\mu\| \leq \kappa_\mu \mu$ in the non-noisy setting, while Condition C2 is the perturbed complementarity condition, similar to the non-noisy setting. However, it is not clear that Condition C2 can always be satisfied since the noise might lead to erratic changes in $X_k^\mu z_k^\mu$. Hence, after satisfying Condition C1, we impose a limit N_μ on the

number of iterations to attempt to satisfy Condition C2 before proceeding to decrease the μ . Using this heuristic, the issue that we observed in Figure 9 is resolved as it is demonstrated in Figure 10. In comparison to Figure 9, Figure 10 demonstrates a more gradual decrease in the barrier parameter. Using this heuristic the algorithm stops in iteration 36 where $\|x_{j,\mathcal{A}_s} - x_{*,\mathcal{A}_s}\|_\infty$ equals 10^{-8} . Thus running the algorithm further does not improve the accuracy of the solution.

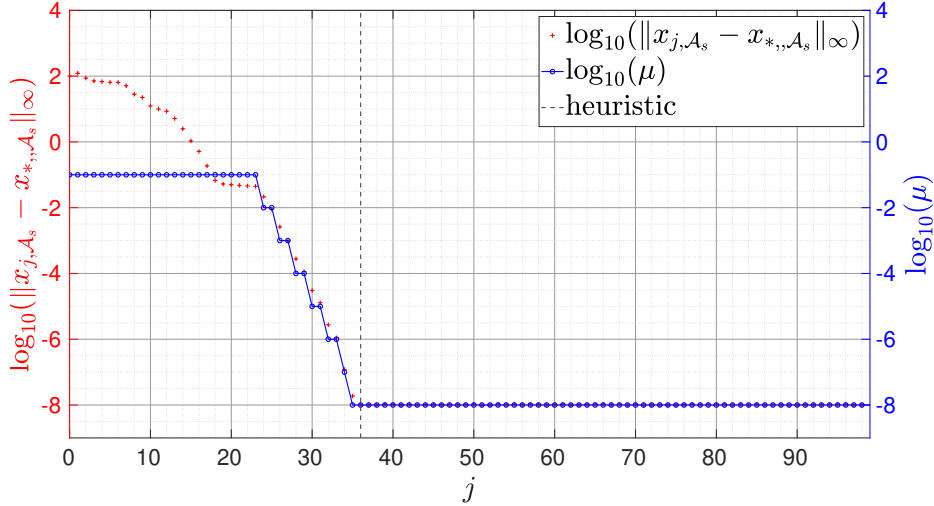


Figure 10: $\log_{10}(\|x_{j,\mathcal{A}_s} - x_{*,\mathcal{A}_s}\|_\infty)$ and $\epsilon_f = 10^{-2}$, $\epsilon_g = \epsilon_H = 10^{-1}$ for `harkerp2` (heuristic)

Tables 5 and 6 display the performance of different update heuristics for all problems, for two different noise levels. The barrier parameter is initialized with $\mu_0 = 0.1$ and decreased by a factor of 10 until it reaches the final target value $\bar{\mu} = 10^{-7}$. **Heuristic** refers to the method that we outlined, i.e., satisfying conditions C1 and C2 and using $N_\mu = 10$ as a safeguard to avoid getting stuck. (The maximum number of N_μ per barrier problem was never reached in these experiments.) **Periodic** refers to a method that decreases the barrier parameter every 40 iterations. The header **Stopping Test** refers to the stopping condition provided in Theorem 3.9 as the sole criterion for decreasing the barrier parameter (as in Figure 9).

We observe that strongly active constraints are identified in all instances. In addition, for most problems, $\|\nabla\varphi_{\text{ter}}\|$'s are within a factor of at most 10 of the noise level. For the **Periodic** method, which takes many more iterations than the other strategies, the values for $\|\nabla\varphi_{\text{ter}}\|$ have slightly smaller values compared to those of the other two methods, as one would expect. The strategies **Heuristic** and **Stopping Test** perform very similarly in terms of the number of iterations taken and the final accuracy. The fact that **Stopping Test** does as well as **Heuristic** is an indication that for these instances, the barrier parameter can be reduced very quickly towards the end of the optimization, and the extra safeguard from Condition C2 might not be necessary in these cases.

For some problems, we observed in Table 5 large values of the final (unscaled) norm of the barrier function gradient, reaching values exceeding 10^3 . We attribute this observation to numerical issues but it deserves further investigation. We also note that $\|\nabla\varphi_{\text{ter}}\|$ for **Periodic** is often equal to the gradient noise level ϵ_g . This can be explained by the specific way we generated the random perturbations that are added to obtain the noisy gradient, see Figure 6.

Table 5: Barrier parameter update rule with $\epsilon_f = 10^{-4}$, and $\epsilon_g = \epsilon_H = 10^{-2}$. See Table 1 for the explanation of some of the headers.

Problem	Heuristic			Periodic			Stopping Test		
	ter	$\ x_{\text{ter}, \mathcal{A}_s}\ _\infty$	$\ \nabla\varphi_{\text{ter}}\ $	ter	$\ x_{\text{ter}, \mathcal{A}_s}\ _\infty$	$\ \nabla\varphi_{\text{ter}}\ $	ter	$\ x_{\text{ter}, \mathcal{A}_s}\ _\infty$	$\ \nabla\varphi_{\text{ter}}\ $
biggsb1	19	NA	1.26e-02	280	NA	1.05e-02	14	NA	1.64e-01
chenhark	57	1.60e-07	8.35e-02	280	1.12e-07	1.16e-02	57	1.60e-07	8.35e-02
cvxbqp1	17	8.45e-08	1.32e-01	280	8.33e-08	1.00e-02	17	8.45e-08	1.32e-01
egl	14	1.06e-07	1.60e-01	280	1.27e-07	1.00e-02	14	1.06e-07	1.60e-01
eigena	35	NA	4.23e+03	280	NA	8.12e+03	31	NA	1.84e-01
explin	27	1.30e-08	1.38e-01	280	1.30e-08	4.03e-02	27	1.30e-08	1.38e-01
explin2	27	1.03e-08	1.37e-01	280	1.03e-08	4.03e-02	27	1.03e-08	1.37e-01
expquad	25	1.00e-08	4.30e-02	280	1.00e-08	1.00e-02	25	1.00e-08	4.30e-02
harkerp2	28	1.15e-07	8.72e-01	280	1.00e-07	9.99e-03	27	1.81e-07	3.20e+00
mccormck	16	1.07e-07	1.00e-02	280	1.07e-07	1.00e-02	16	1.07e-07	1.00e-02
mdhole	41	1.19e-07	1.53e-01	280	1.01e-07	1.00e-02	41	1.19e-07	1.53e-01
ncvxbqp1	65	1.92e-06	1.34e-01	280	1.98e-06	1.00e-02	65	1.92e-06	1.34e-01
ncvxbqp2	114	2.08e-06	2.42e-01	280	1.98e-06	1.00e-02	114	2.08e-06	2.42e-01
ncvxbqp3	165	3.23e-05	1.43e-01	280	2.96e-05	1.00e-02	163	5.75e-05	3.95e+03
nonscomp	23	NA	1.62e-02	280	NA	1.03e-02	20	NA	1.22e-01
obstclal	20	3.49e-06	1.07e-02	280	3.78e-06	1.00e-02	19	4.60e-06	1.23e-01
obstclbl	19	3.90e-06	1.27e-01	280	4.61e-06	1.00e-02	19	3.90e-06	1.27e-01
obstclbu	19	3.90e-06	1.27e-01	280	4.61e-06	1.00e-02	19	3.90e-06	1.27e-01
pentdi	24	4.02e-07	1.17e-02	280	4.02e-07	1.02e-02	23	3.92e-07	9.94e-02
qrtquad	28	1.01e-08	2.70e-02	280	1.01e-08	1.00e-02	28	1.01e-08	2.70e-02
qudlin	36	1.00e-08	1.46e+00	280	1.00e-08	5.38e-02	29	1.00e-08	1.26e-01
sim2bqp	14	7.92e-08	2.62e-01	280	1.01e-07	9.98e-03	14	7.92e-08	2.62e-01

Table 6: Barrier parameter update rule with $\epsilon_f = 10^{-6}$, and $\epsilon_g = \epsilon_H = 10^{-3}$. See Table 1 for the explanation of some of the headers.

Problem	Heuristic			Periodic			Stopping Test		
	ter	$\ x_{\text{ter}, \mathcal{A}_s}\ _\infty$	$\ \nabla\varphi_{\text{ter}}\ $	ter	$\ x_{\text{ter}, \mathcal{A}_s}\ _\infty$	$\ \nabla\varphi_{\text{ter}}\ $	ter	$\ x_{\text{ter}, \mathcal{A}_s}\ _\infty$	$\ \nabla\varphi_{\text{ter}}\ $
biggsb1	22	NA	1.23e-03	280	NA	5.62e-04	18	NA	2.49e+00
chenhark	323	1.70e-07	1.93e-02	280	1.15e-07	1.67e-03	323	1.70e-07	1.93e-02
cvxbqp1	22	8.33e-08	1.00e-03	280	8.33e-08	1.00e-03	22	8.33e-08	1.00e-03
egl	17	1.28e-07	2.26e-03	280	1.28e-07	1.00e-03	17	1.28e-07	2.26e-03
eigena	39	NA	1.63e-02	280	NA	1.00e-03	38	NA	5.49e-02
explin	29	1.30e-08	3.88e-02	280	1.30e-08	3.88e-02	29	1.30e-08	3.88e-02
explin2	30	1.03e-08	3.88e-02	280	1.03e-08	3.88e-02	30	1.03e-08	3.88e-02
expquad	29	1.00e-08	4.50e-03	280	1.00e-08	1.00e-03	29	1.00e-08	4.50e-03
harkerp2	33	1.00e-07	1.09e-03	280	1.00e-07	1.00e-03	33	1.00e-07	1.09e-03
mccormck	19	1.07e-07	1.04e-03	280	1.07e-07	1.00e-03	19	1.07e-07	1.04e-03
mdhole	40	9.83e-08	1.65e-02	280	1.00e-07	1.00e-03	40	9.83e-08	1.65e-02
ncvxbqp1	65	1.97e-06	1.12e-03	280	1.97e-06	1.16e-03	65	1.97e-06	1.12e-03
ncvxbqp2	122	1.97e-06	1.07e-03	280	1.97e-06	1.06e-03	122	1.97e-06	1.07e-03
ncvxbqp3	163	2.78e-05	1.03e-03	280	2.81e-05	1.04e-03	163	2.78e-05	1.03e-03
nonscomp	26	NA	1.26e-02	280	NA	9.99e-04	22	NA	7.15e-02
obstclal	24	3.56e-06	1.00e-03	280	3.56e-06	1.00e-03	24	3.56e-06	1.00e-03
obstclbl	23	4.34e-06	9.98e-04	280	4.36e-06	1.00e-03	23	4.34e-06	9.98e-04
obstclbu	23	4.34e-06	9.98e-04	280	4.36e-06	1.00e-03	23	4.34e-06	9.98e-04
pentdi	31	4.01e-07	1.07e-03	280	4.01e-07	9.99e-04	31	4.01e-07	1.07e-03
qrtquad	30	1.01e-08	3.19e-03	280	1.01e-08	1.00e-03	30	1.01e-08	3.19e-03
qudlin	44	9.99e-09	4.84e-02	280	1.00e-08	1.68e-01	37	9.67e-07	1.83e+03
sim2bqp	18	9.91e-08	9.24e-03	280	1.00e-07	1.00e-03	18	9.91e-08	9.24e-03